Supporting Information

High-Rate Fingerprinting of Protein Isoforms by Quasi-regulated Enzyme-free Transport Through CytK Nanopores

Amr Makhamreh[1], Ali Fallahi[1], Rik Dhar[2], Monika Kumari[3], Siddharth Krishnan[3], Michele Meseonznik[1], Luning Yu[2], Dina Boyko[2], Keira Reich-Veillette[1], Yuhaohua Zheng[2], Elizabeth A. Libby[1], Aleksei Aksimentiev[3], and Meni Wanunu[1, 2#]

[1]*Dept. of Bioengineering, Northeastern University, Boston, MA*

[2]*Dept. of Physics, Northeastern University, Boston, MA*

[3]*Dept. of Physics, University of Illinois at Urbana-Champaign, Urbana, IL*

[#]*Corresponding author.*

wanunu@neu.edu

Supporting Information

Table of Contents

Figure S1. Gating characteristics of CytK at -200 mV in 1M KCl, 2M GdmCl, 10mM Tris, pH 7.5. 3

Figure S2. High event rate with trans-to-cis translocation of MBP through CytK at 150 nM. 3

Figure S3. Trans-to-cis blockade events of MBP-WT with CytK at -200 mV and -300 mV in 1M KCl, 2M GdmCl, 10mM Tris, pH 7.5. 4

Figure S4. Higher versus lower fractional blockade trans-to-cis translocation events of MBP-D10 through CytK. 5

Figure S5. MD simulations of CytK conductivity. 6

Figure S6. Ionic current through peptide-blocked CytK nanopore. 7

Figure S7. SDS PAGE of purified PBI analytes. 8

Figure S8. Fractional blockade versus dwell time of trans-to-cis translocation of P1 through CytK. 9

Figure S9. Fractional blockade versus dwell time of trans-to-cis translocation of P2 through CytK. 10

Figure S10. Fractional blockade versus dwell time of trans-to-cis translocation of P3 through CytK. 11

Figure S11. Fractional blockade versus dwell time of trans-to-cis translocation of P4 through CytK. 12

Figure S12. MBP reverse translocation signals as a function of voltage. 13

Figure S13. P1 reverse translocation signals as a function of voltage. 14

Figure S14. P2 reverse translocation signals as a function of voltage. 15

Figure S15. P3 reverse translocation signals as a function of voltage. 16

Figure S17. Correlation of number of detected segments in events and their duration at –300 mV. 18

Figure S18. Histograms of event segment counts and durations at -300 mV. 19

Figure S19. Clustering results on DTW Distance matrix of MBP Events and barycenters of clusters. 20

Figure S20. Clustering results on DTW Distance matrix of P1 Events and barycenters of clusters. 21

Figure S21. Clustering results on DTW Distance matrix of P2 Events and barycenters of clusters. 21

Figure S22. Clustering results on DTW Distance matrix of P3 Events and barycenters of clusters. 22

Figure S23. Clustering results on DTW Distance matrix of P4 Events and barycenters of clusters. 22

Figure S24. Two trials of multi-resolution simulation of full-length protein translocation and the resulting ionic current. 23

Figure S25. Total current distribution from high duty cycle measurements under saturated concentrations. 24

Figure S26. Soft-DTW score threshold used for discrimination of P2 translocations from background events in cell lysate. 25

Sequences and plasmid designs for PBI analytes 25

Table 1: MBP and PBI analytes amino acid sequences. 25

Table 2: MBP and PBI analytes DNA sequences. 27

Table 3: MBP and PBI analytes normalized reverse capture rates ($nM^{-1}s^{-1}$) versus voltage. 30

Table 4: Intact mass spectrometry results on PBIs.....30

Table 5: Signal segment statistics for PBI analytes. 30

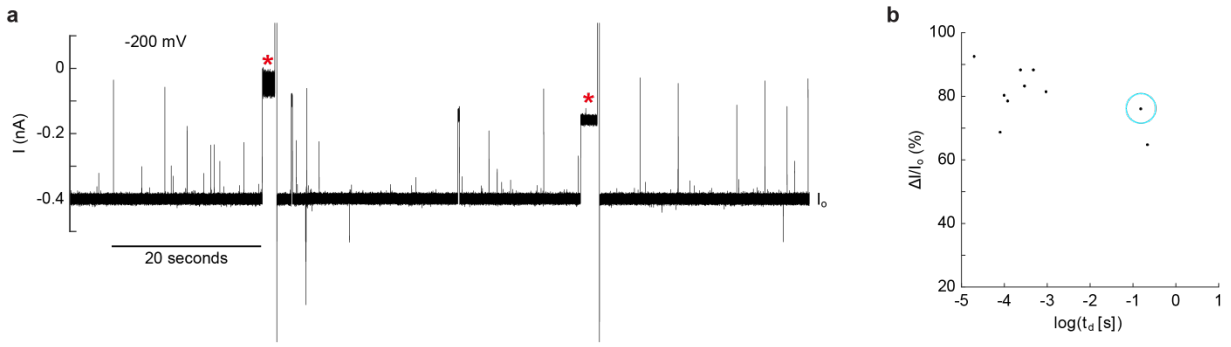

Figure S1. Gating characteristics of CytK at -200 mV in 1M KCl, 2M GdmCl, 10mM Tris, pH 7.5. a, Open-pore baseline (I_o) recording of CytK at -200 mV with no analyte present in the *trans* chamber. Red asterisks indicate long-lived gating events that required a voltage reversal (+200 mV) for pore reset back to I_o. **b,** Fractional blockade versus dwell time of transient gating events in the control trace in **a**. The circled event (cyan) was a false-positive (FP) event that met the conditions for the first stage of our event extraction pipeline.

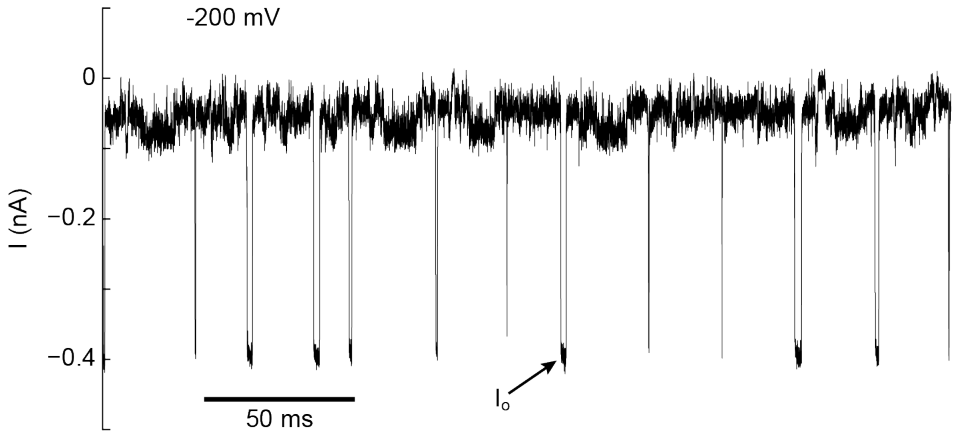

Figure S2. High event rate with trans-to-cis translocation of MBP through CytK at 150 nM. Continuous trace showing reverse translocation of MBP through CytK at a concentration of 150 nM. The applied voltage is -200 mV and the arrow points to the short instances where I_o is observed between MBP translocation events.

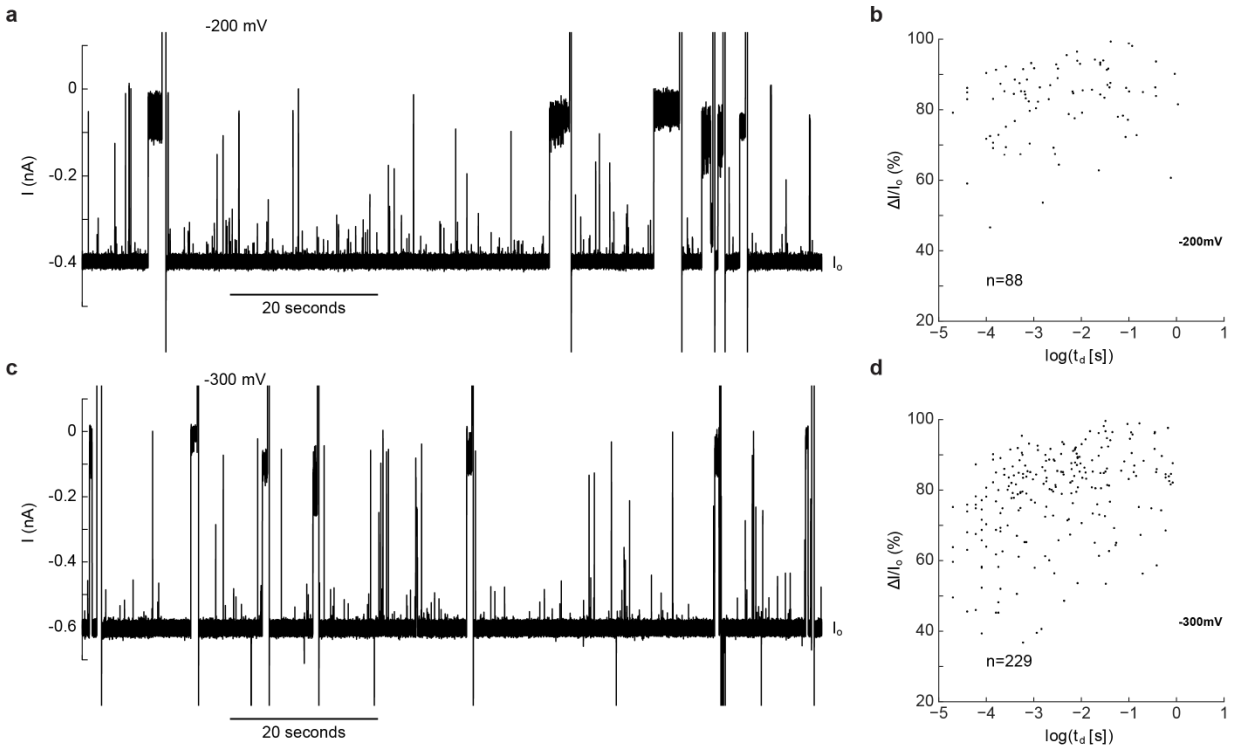

Figure S3. *Trans*-to-*cis* blockade events of MBP-WT with CytK at -200 mV and -300 mV in 1M KCl, 2M GdmCl, 10mM Tris, pH 7.5. a, Continuous (100 seconds) recording of CytK at -200 mV with 5 nM of MBP-WT present in the *trans* chamber. Open-pore baseline is denoted as I_o and capacitive spikes indicate the application of a reverse potential (+200 mV) to remove long-lived clogging events to open the pore back to I_o. **b,** Fractional blockade versus dwell time of transient events in observed with CytK when 5 nM of MBP-WT is present in the *trans* chamber at -200 mV. **c,** Continuous (100 seconds) recording of CytK at -300 mV with 5 nM of MBP-WT present in the *trans* chamber. Open-pore baseline is denoted as I_o and capacitive spikes indicate the application of a reverse potential (+300 mV) to remove long-lived clogging events to open the pore back to I_o. **d,** Fractional blockade versus dwell time of transient events in observed with CytK when 5 nM of MBP-WT is present in the *trans* chamber at -300 mV.

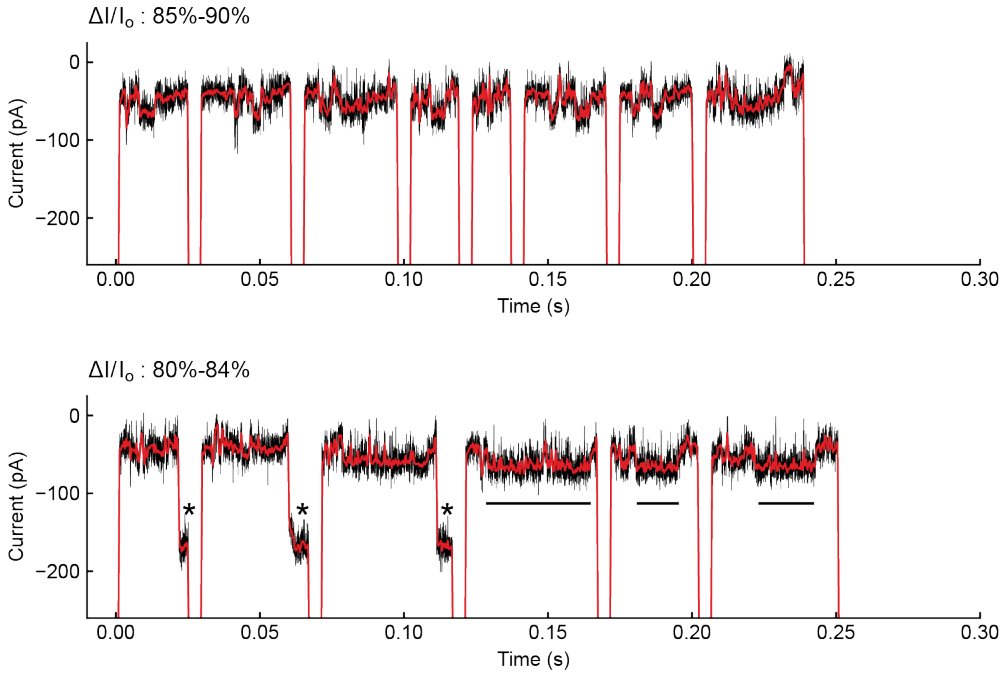

Figure S4. Higher versus lower fractional blockade *trans*-to-*cis* translocation events of MBP-D10 through CytK. Example reverse translocation events of MBP through the *trans* side of CytK at -175 mV. Top shows translocation events with a mean ΔI/Io between than 85% and 90%. Bottom shows translocation events with a mean ΔI/Io between than 80% and 84%. Events with asterisks (left) exhibit a shallow blockade level prior to the end of the event. Events with horizontal lines (right) have the shallow blockade level within the transport signal of MBP extended for a longer duration compared to the events shown on top.

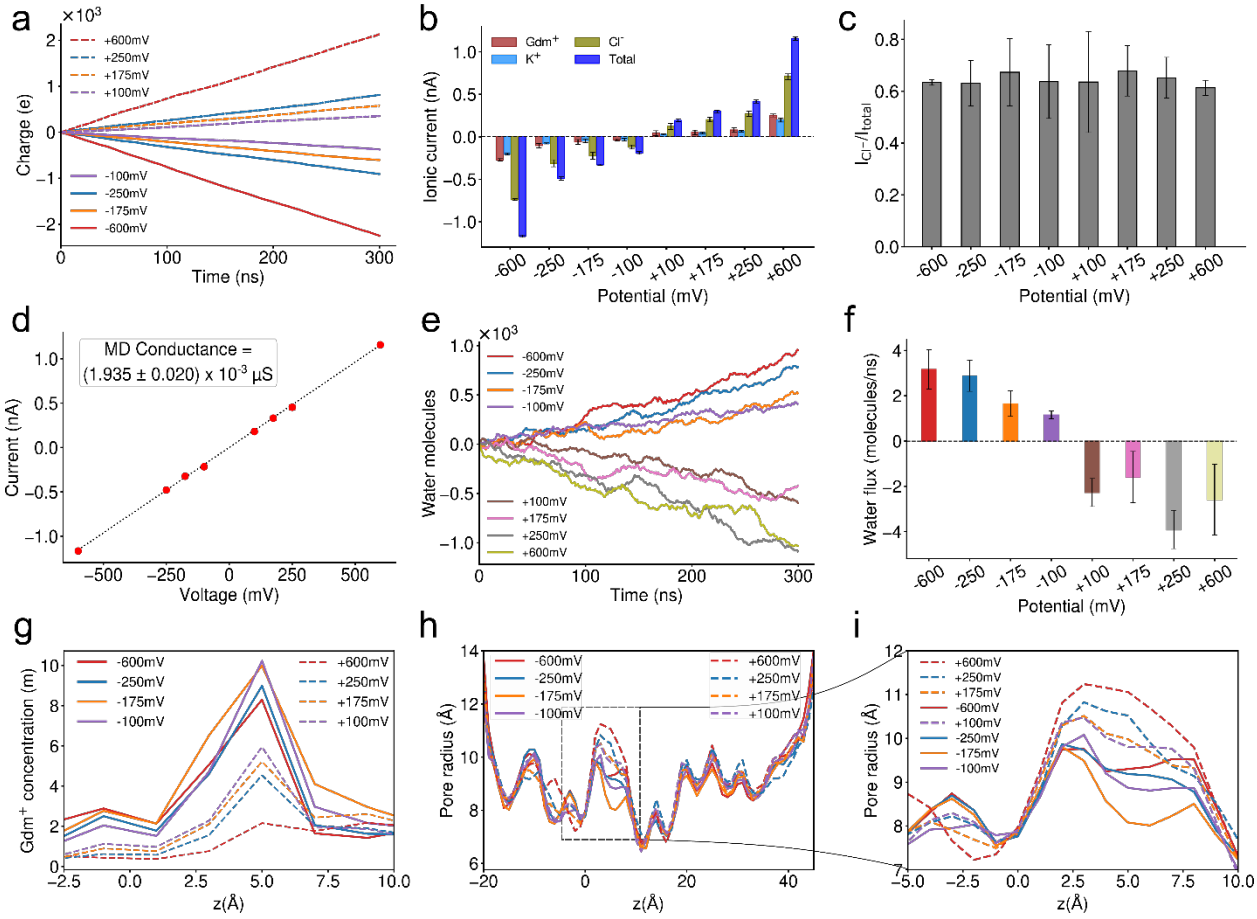

Figure S5. MD simulations of CytK conductivity. a, Cumulative charge carried by all ions through a CytK nanopore in MD simulations carried out at specified transmembrane voltage and a 2 M GdmCl / 1 M KCl electrolyte mixture. **b,** Average current carried by the ionic species and the total average current. **c,** The fraction of the total average current carried by Cl- ions. **d,** Simulated conductance of CytK nanopore computed as the slope of the current-voltage curve. The associated error was estimated using weighted least-square fitting with each data point weighted considering the error in the current measurements. **e,** Number of water molecules that passed through the nanopore in the MD simulations at specified bias conditions. **f,** Average water flux calculated as the slope of the water passage curves excluding the first 50 ns of each simulation. In panels e and f, the error bars show the standard error of mean computed by splitting the MD trajectories into 30 ns fragments. **g,** Zoomed-in view of the distributions of Gdm+ ions near the Lys130 and Glu141 residues of the nanopore. **h,** Local radius of CytK nanopore at specified bias conditions. The local radius was determined in 1 Å bins by calculating the ratio of water oxygens (nw) to non-hydrogen nanopore and Gdm+ atoms (np) in cylindrical segments of increasing radius. The local nanopore radius was defined as the radius of the cylinder at which nw/np becomes less then 0.5. **i,** Zoomed-in view of the pore radius near the Lys130 and Glu141 residues of the nanopore.

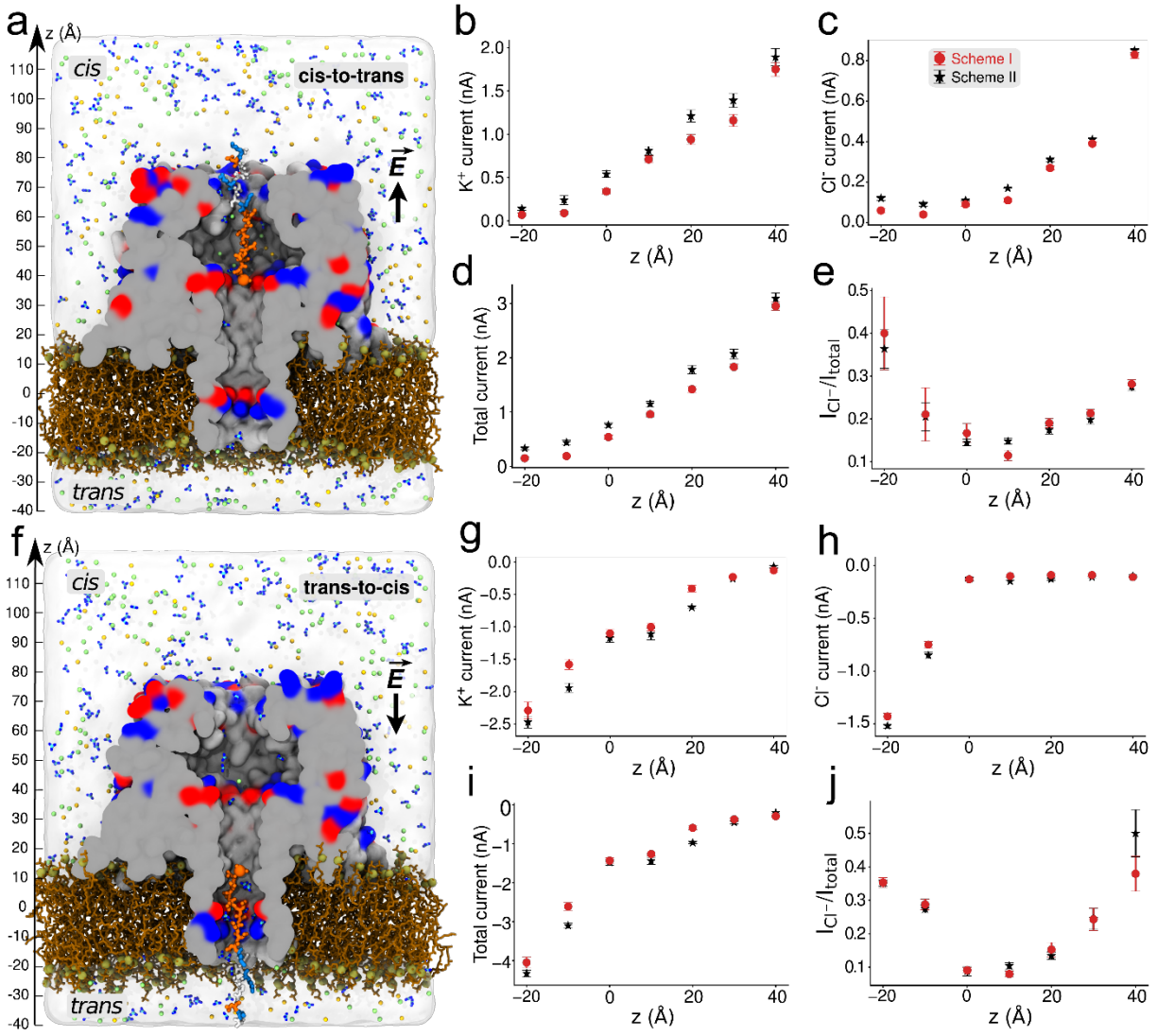

Figure S6. Ionic current through peptide-blocked CytK nanopore. a, Initial configuration of one simulation system (at z = 40 Å) where the peptide is oriented in the "cis-to-trans" translocation direction. Three replica per systems were simulated in parallel for each configuration at +1.2 V differing by the placement of the peptide (in 10 Å increments) and the peptide restrain method (Scheme I, red and Scheme II, black). The analyte peptide is color-coded according to amino acid charge: anionic in orange, cationic in blue, and uncharged in silver. **b-d**, Average current of K+ and Cl- ions and the total ionic currents for various locations of the peptide's first residue Ca atom (orange sphere in panel a). Total current includes ionic current generated by the movement of K+, Cl-, and Gdm+ ions. For each data point, the error bar shows the standard error of mean computed by splitting three independent 210 ns MD trajectories into 30 ns fragments. **e,** Fraction of total current carried by chloride ions. **f-j**, Same as in panels a-e but for the "trans-to-cis" translocation direction.

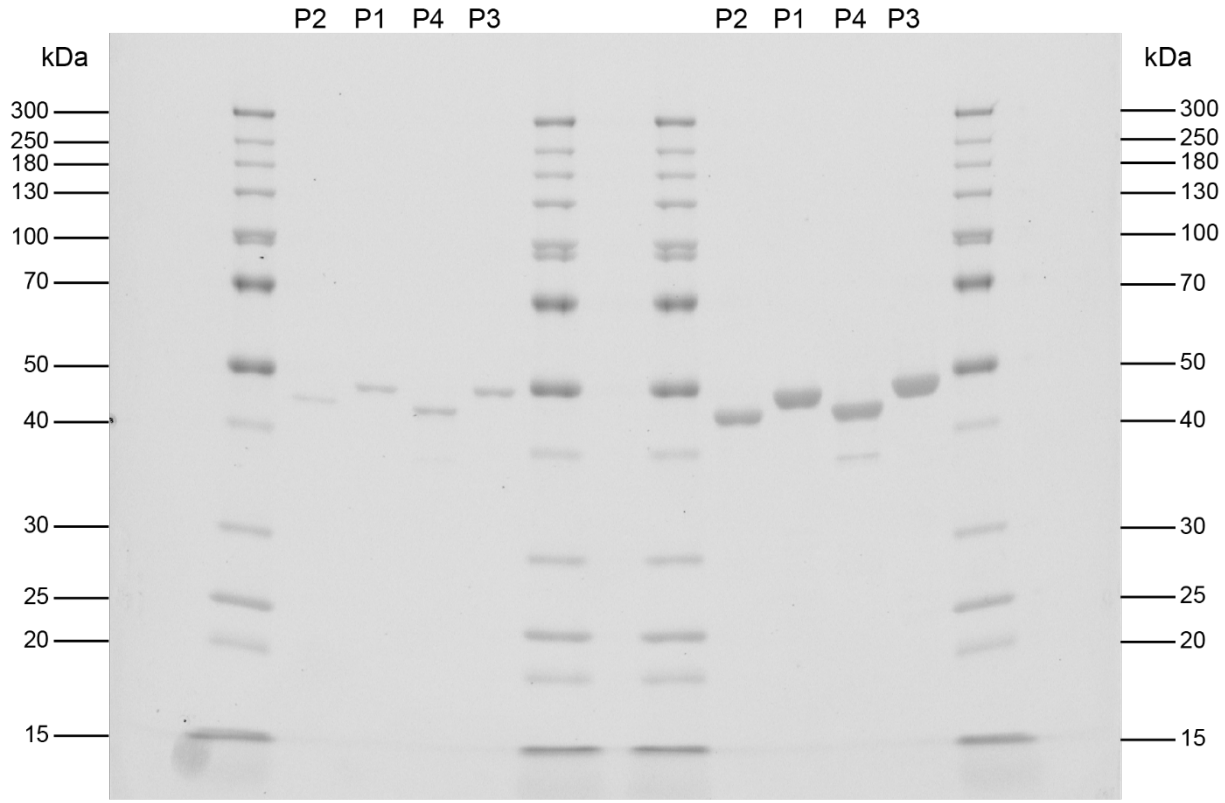

Figure S7. SDS PAGE of purified PBI analytes. Shown is a 12% Tris-glycine SDS PAGE of purified stocks of PBI analytes. Each analyte was loaded at 0.2 ng (left) and 1 ng (right).

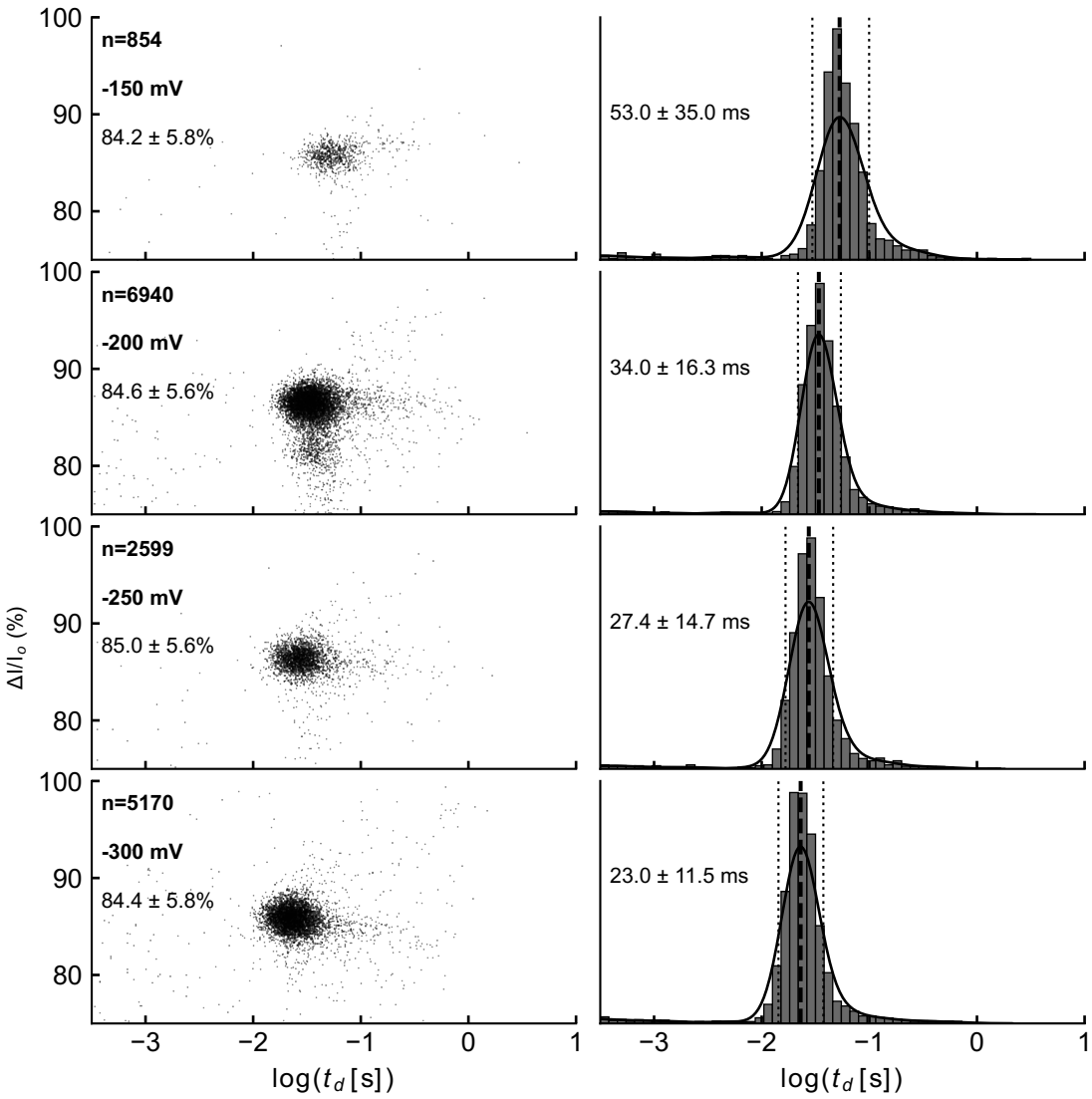

Figure S8. Fractional blockade versus dwell time of *trans*-to-*cis* translocation of P1 through CytK. Shown on the left are scatter plots of the fractional blockade (ΔI/Io) versus log(t_d) of reverse P1 translocation events through the *trans* side of CytK. For each scatter, the voltage, sample size, and μ±σ are provided. Shown on the right are the distributions for the log(t_d) of MBP translocation events, with each dwell time histogram corresponding to the scatter plot on the left. Dwell time histograms are fit with a Gaussian kernel-density estimate (KDE), where the full width half maximum (FWHM) of the KDE fit are shown as the thin dashed lines and the KDE mode of each distribution is shown as the thick black line overlaid on the histogram. The KDE mode±FWHM at each voltage is provided.

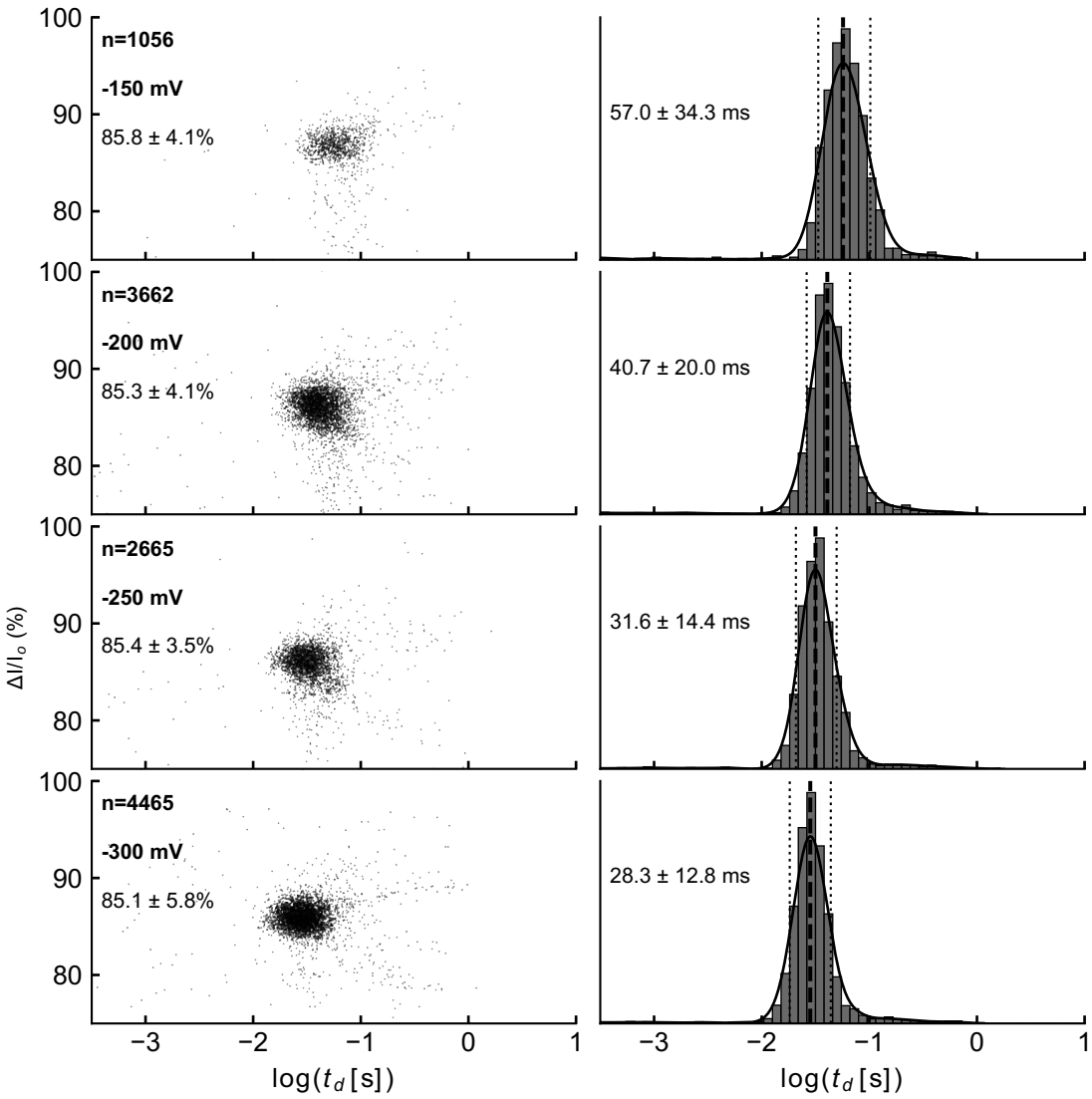

Figure S9. Fractional blockade versus dwell time of *trans*-to-*cis* translocation of P2 through CytK. Shown on the left are scatter plots of the fractional blockade (ΔI/Io) versus log(t_d) of reverse P2 translocation events through the *trans* side of CytK. For each scatter, the voltage, sample size, and μ±σ are provided. Shown on the right are the distributions for the log(t_d) of MBP translocation events, with each dwell time histogram corresponding to the scatter plot on the left. Dwell time histograms are fit with a Gaussian kernel-density estimate (KDE), where the full width half maximum (FWHM) of the KDE fit are shown as the thin dashed lines and the KDE mode of each distribution is shown as the thick black line overlaid on the histogram. The KDE mode±FWHM at each voltage is provided.

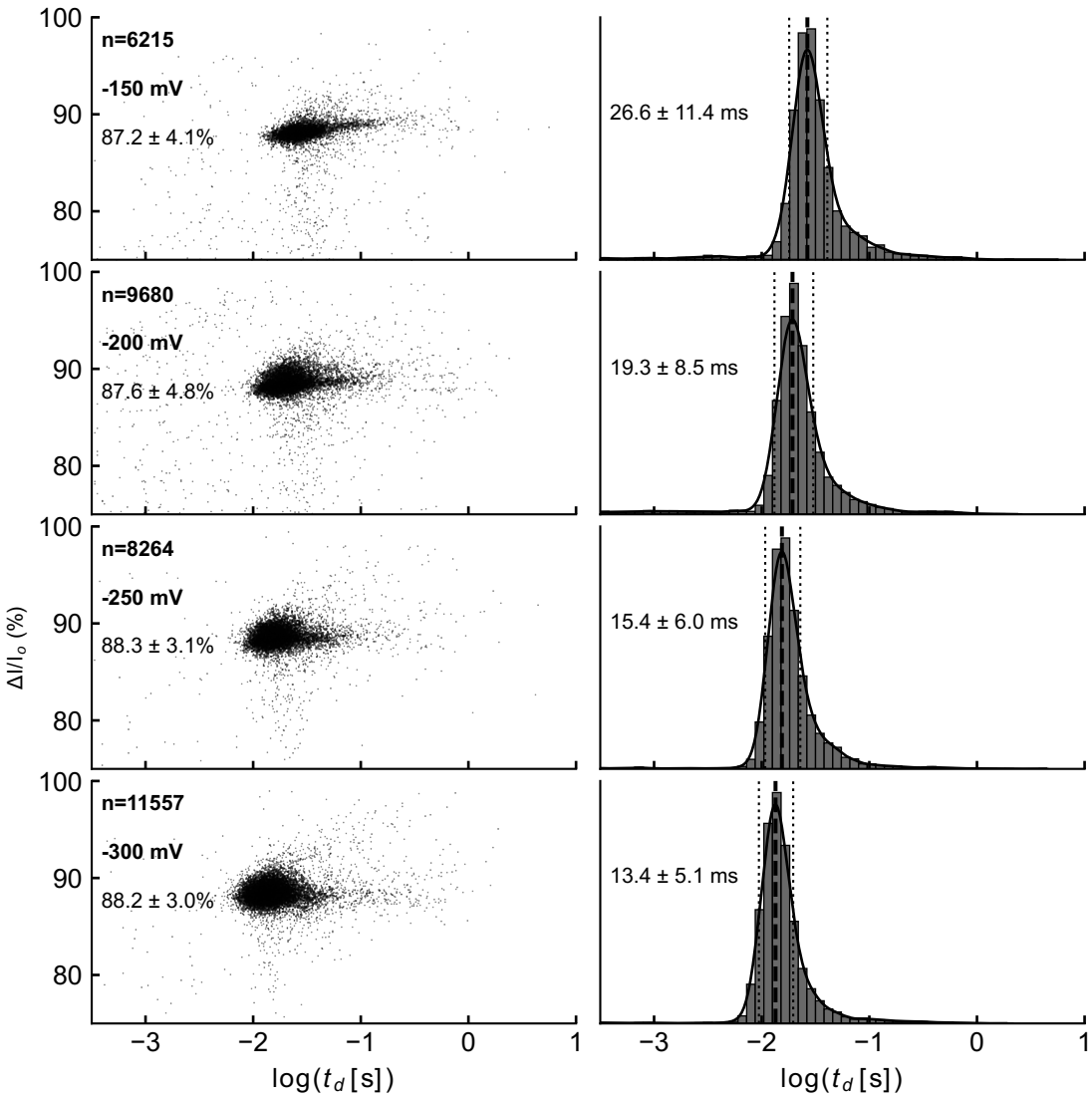

Figure S10. Fractional blockade versus dwell time of *trans*-to-*cis* translocation of P3 through CytK. Shown on the left are scatter plots of the fractional blockade (ΔI/Io) versus log(t_d) of reverse P3 translocation events through the *trans* side of CytK. For each scatter, the voltage, sample size, and μ±σ are provided. Shown on the right are the distributions for the log(t_d) of MBP translocation events, with each dwell time histogram corresponding to the scatter plot on the left. Dwell time histograms are fit with a Gaussian kernel-density estimate (KDE), where the full width half maximum (FWHM) of the KDE fit are shown as the thin dashed lines and the KDE mode of each distribution is shown as the thick black line overlaid on the histogram. The KDE mode±FWHM at each voltage is provided.

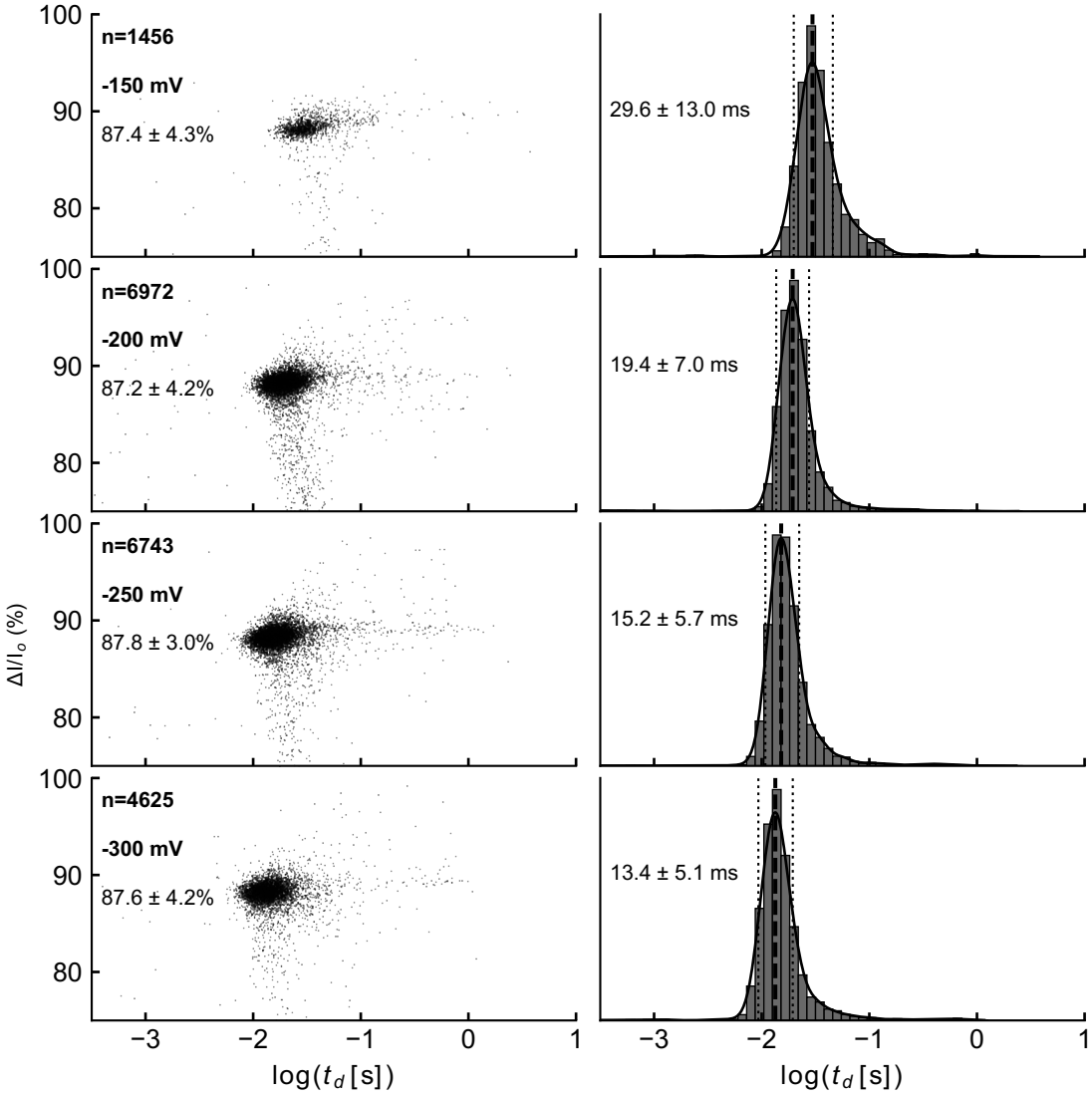

Figure S11. Fractional blockade versus dwell time of *trans*-to-*cis* translocation of P4 through CytK. Shown on the left are scatter plots of the fractional blockade (ΔI/Io) versus log(t_d) of reverse P4 translocation events through the *trans* side of CytK. For each scatter, the voltage, sample size, and μ±σ are provided. Shown on the right are the distributions for the log(t_d) of MBP translocation events, with each dwell time histogram corresponding to the scatter plot on the left. Dwell time histograms are fit with a Gaussian kernel-density estimate (KDE), where the full width half maximum (FWHM) of the KDE fit are shown as the thin dashed lines and the KDE mode of each distribution is shown as the thick black line overlaid on the histogram. The KDE mode±FWHM at each voltage is provided.

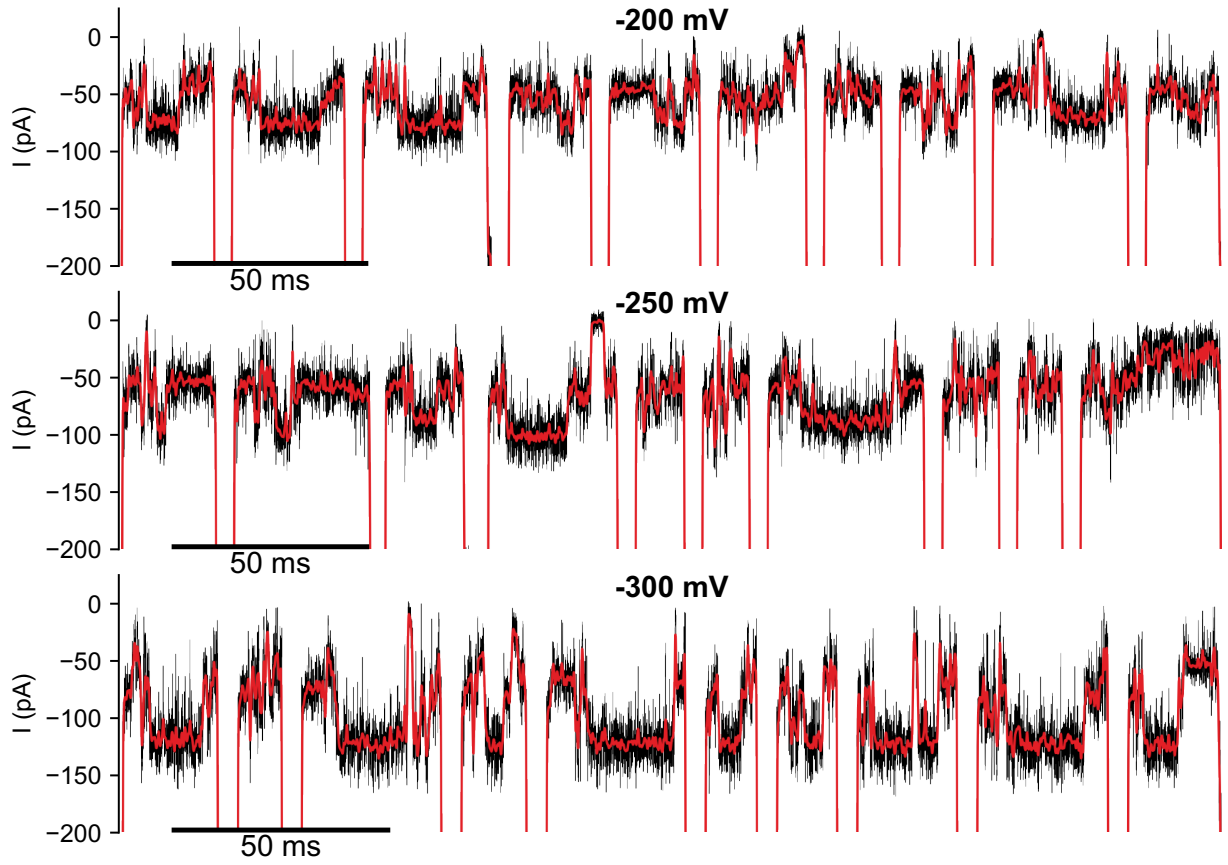

Figure S12. MBP reverse translocation signals as a function of voltage. Example reverse translocation events of MBP through the *trans* side of CytK at –200 (top), –250 (middle), and –300 (bottom) mV. Each event is shown using 1.5 kHz digital low-pass filtered signal (red) overlaid onto the 25 kHz signal (black).

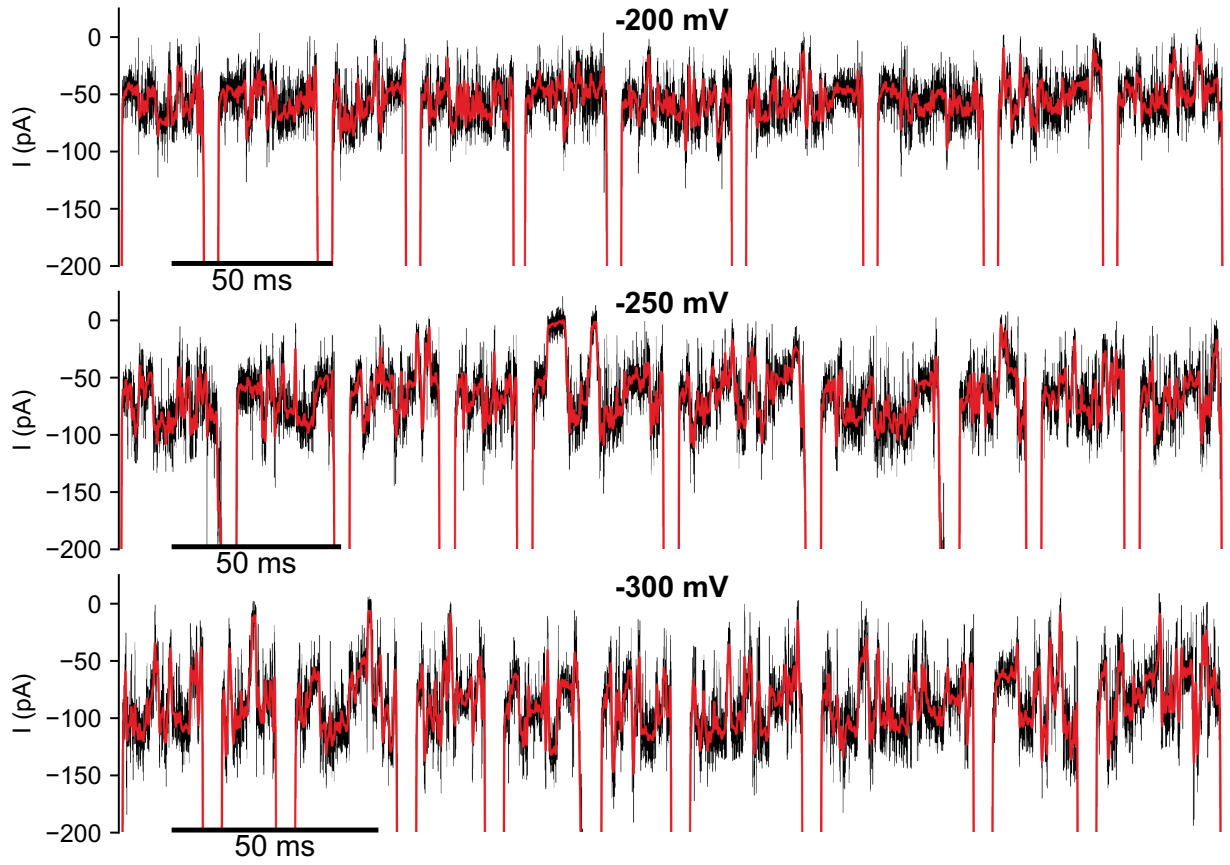

Figure S13. P1 reverse translocation signals as a function of voltage. Example reverse translocation events of P1 through the *trans* side of CytK at –200 (top), –250 (middle), and –300 (bottom) mV. Each event is shown using 1.5 kHz digital low-pass filtered signal (red) overlaid onto the 25 kHz signal (black).

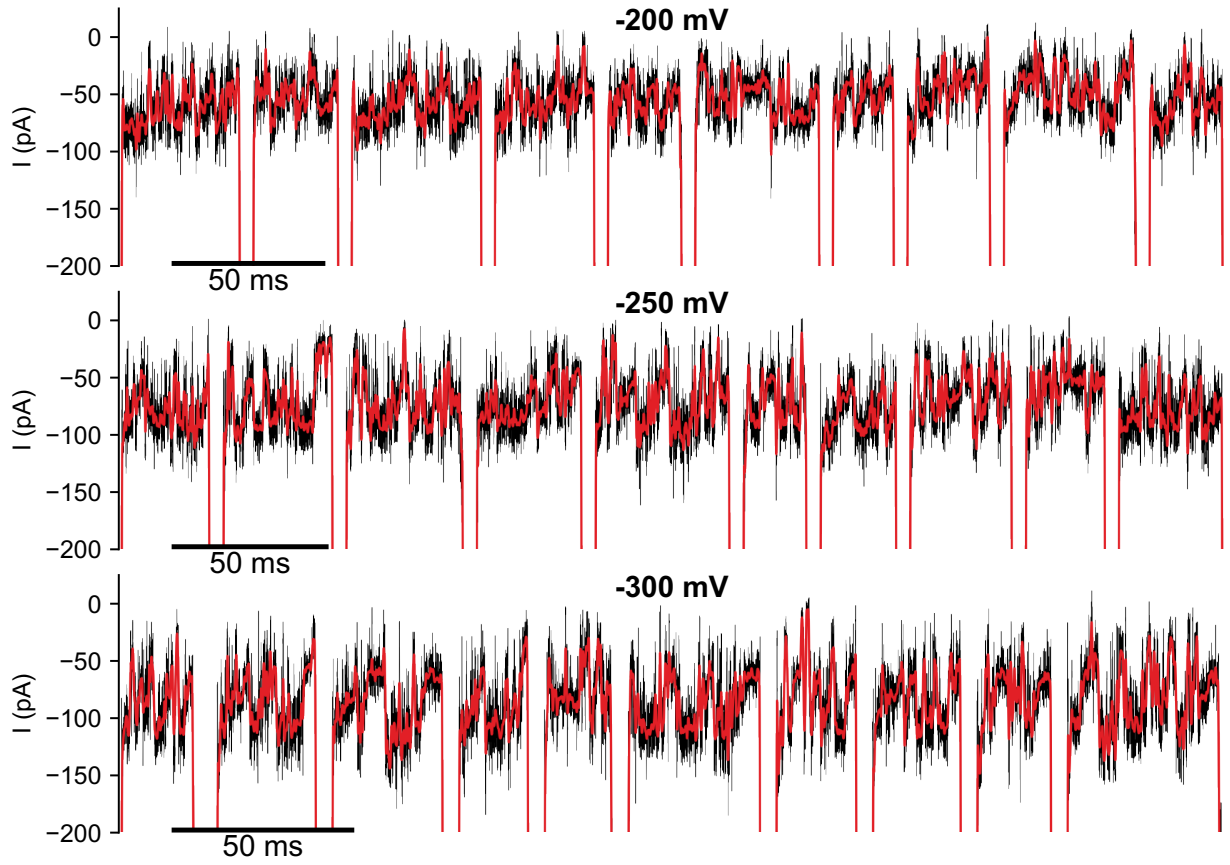

Figure S14. P2 reverse translocation signals as a function of voltage. Example reverse translocation events of P2 through the *trans* side of CytK at –200 (top), –250 (middle), and –300 (bottom) mV. Each event is shown using 1.5 kHz digital low-pass filtered signal (red) overlaid onto the 25 kHz signal (black).

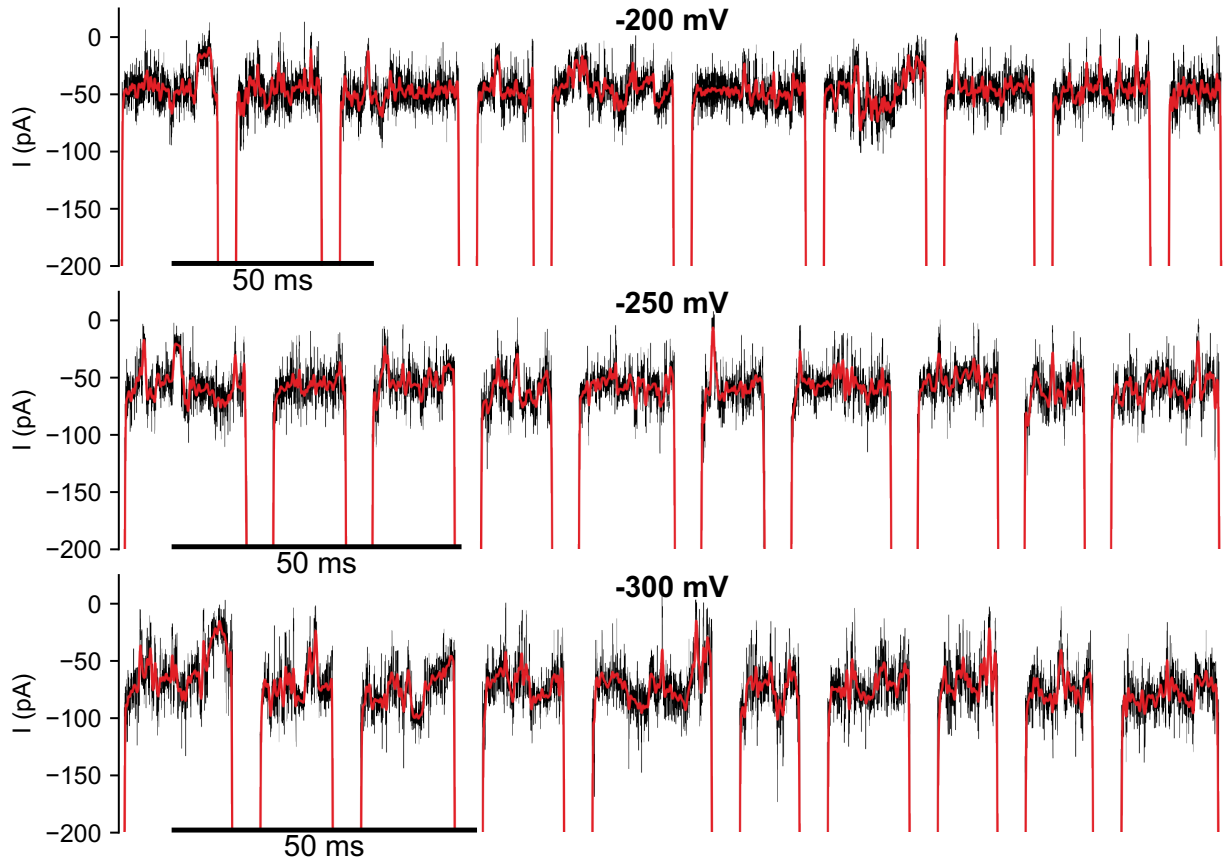

Figure S15. P3 reverse translocation signals as a function of voltage. Example reverse translocation events of P3 through the *trans* side of CytK at –200 (top), –250 (middle), and –300 (bottom) mV. Each event is shown using 1.5 kHz digital low-pass filtered signal (red) overlaid onto the 25 kHz signal (black).

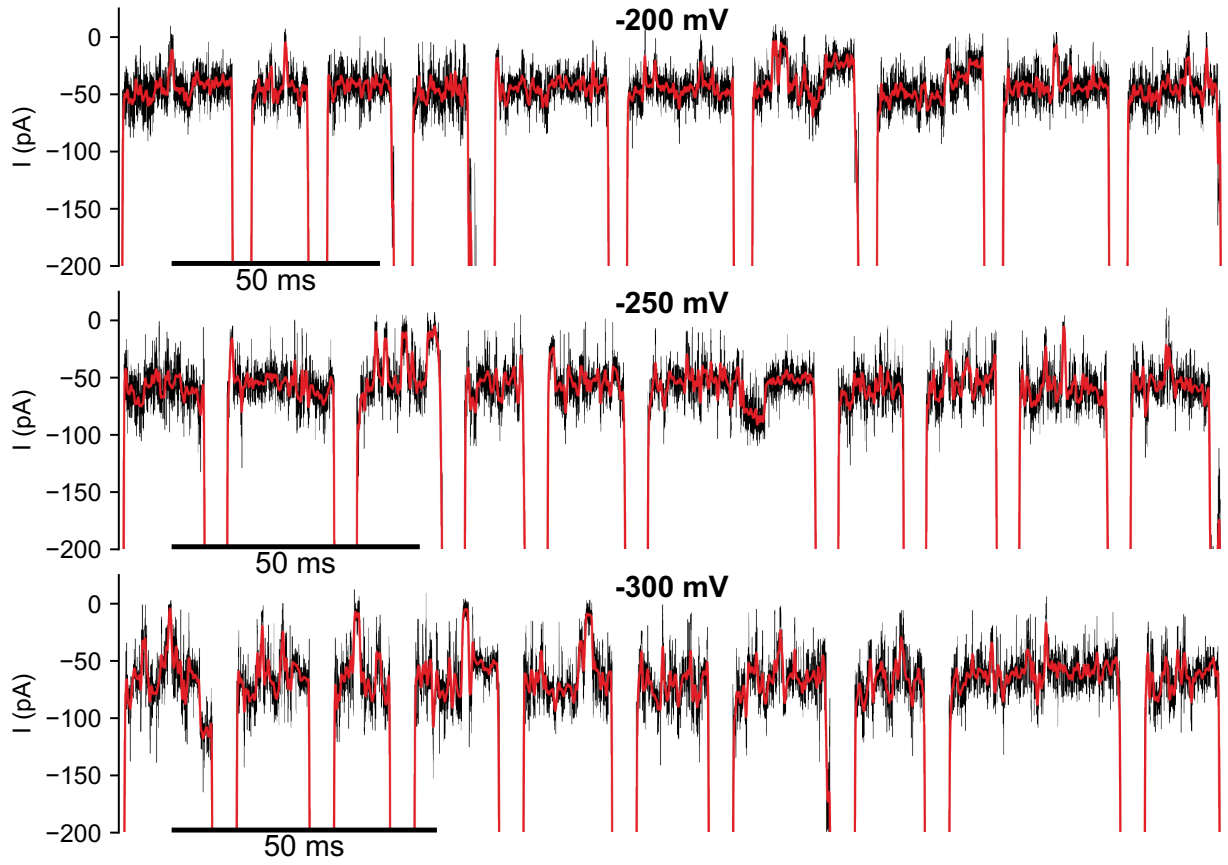

Figure S16. P4 reverse translocation signals as a function of voltage. Example reverse translocation events of P4 through the *trans* side of CytK at –200 (top), –250 (middle), and –300 (bottom) mV. Each event is shown using 1.5 kHz digital low-pass filtered signal (red) overlaid onto the 25 kHz signal (black).

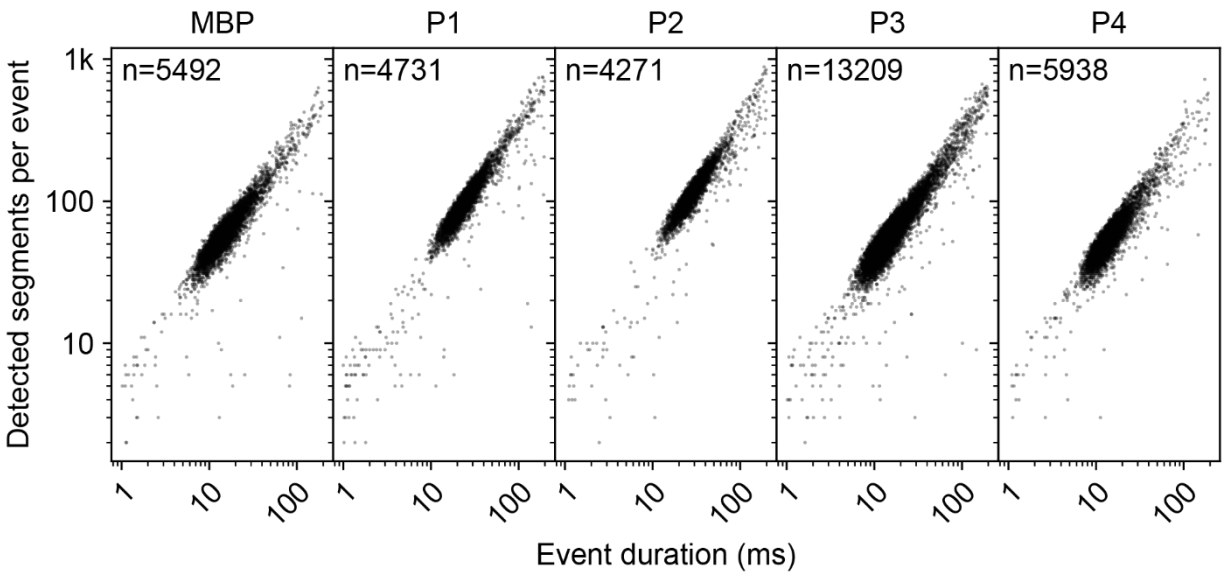

Figure S17. Correlation of number of detected segments in events and their duration at –300 mV. Identical parameters for Bayesian Segmentation were used for all different protein types (min. segment length = 5 samples (100 µs), window size = 500 samples (10 ms), false positive rate = 5000 segments/second). The resulting segments were then merged iteratively by dwell-time-weighted averaging, starting from the lowest-difference segments, until all consecutive segments were at least 5 pA apart.

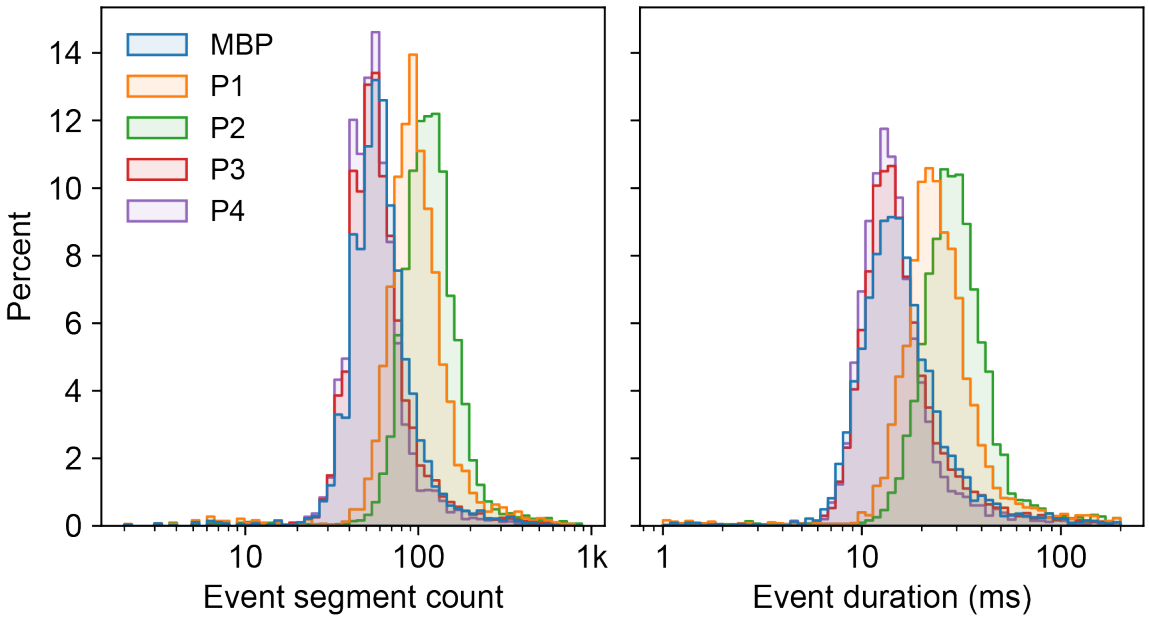

Figure S18. Histograms of event segment counts and durations at -300 mV. The histograms were derived from the same data shown in Figure S17. The height of each histogram is normalized independently to add up to 100%. The segment count distributions are narrower than dwell time distributions, which hints at a reduction in the effect of stochastic stalling during translocation.

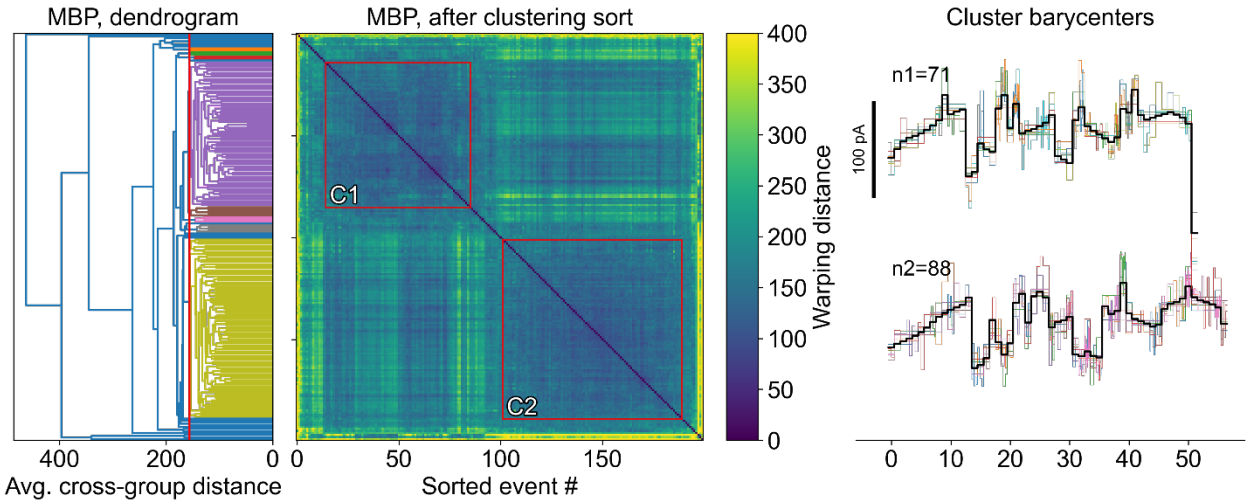

Figure S19. Clustering results on DTW Distance matrix of MBP Events and barycenters of clusters. After UPGMA clustering and sorting according to cross-group average distance, the dendogram and sorted distance matrix yielded shows similar groups of events and outliers. The cutoff line on the dendogram is drawn at the 0.85th quantile of node distances. The resulting subclusters of events (color-coded) were filtered for a minimum size equal to 15% of the population (30 events), yielding two clusters C1 and C2. On the right, the barycenters of the clusters along with 7 randomly selected and aligned events from each cluster are displayed. The clusters appear largely similar, and the main differentiator appears to be the tail end of events of cluster C1 being stuck in the pore and producing a short transient low-blockade level.

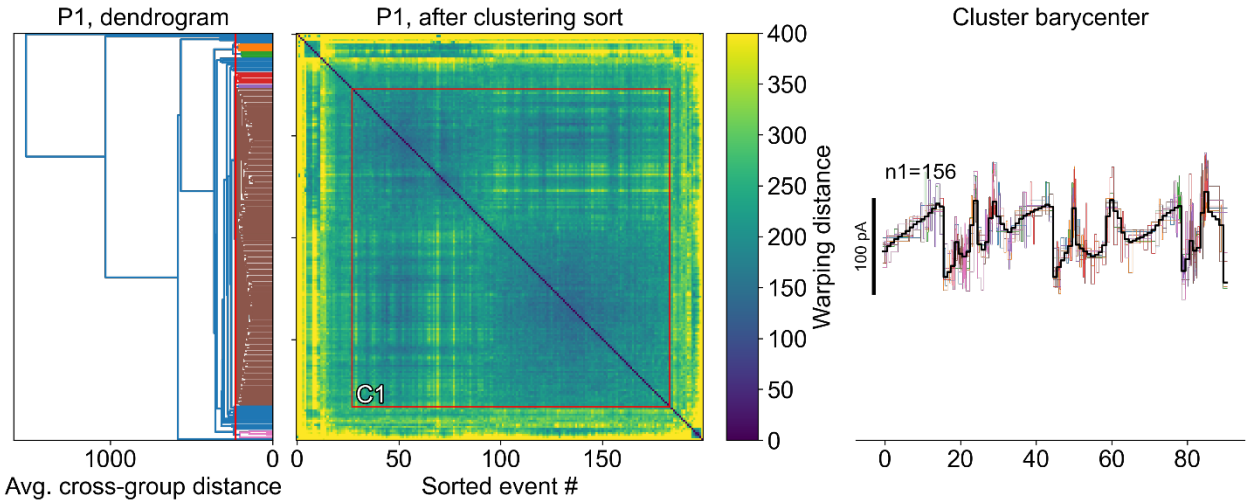

Figure S20. Clustering results on DTW Distance matrix of P1 Events and barycenters of clusters. Refer to Figure S19 for general description. Here, only one large cluster is formed under the same formation and filtration criteria. Based on the distance matrix, two clusters are observed here. For the sake of consistency, the same cut-point criterion based on 0.85th quantile of node distances was chosen, and therefore only one large cluster was formed.

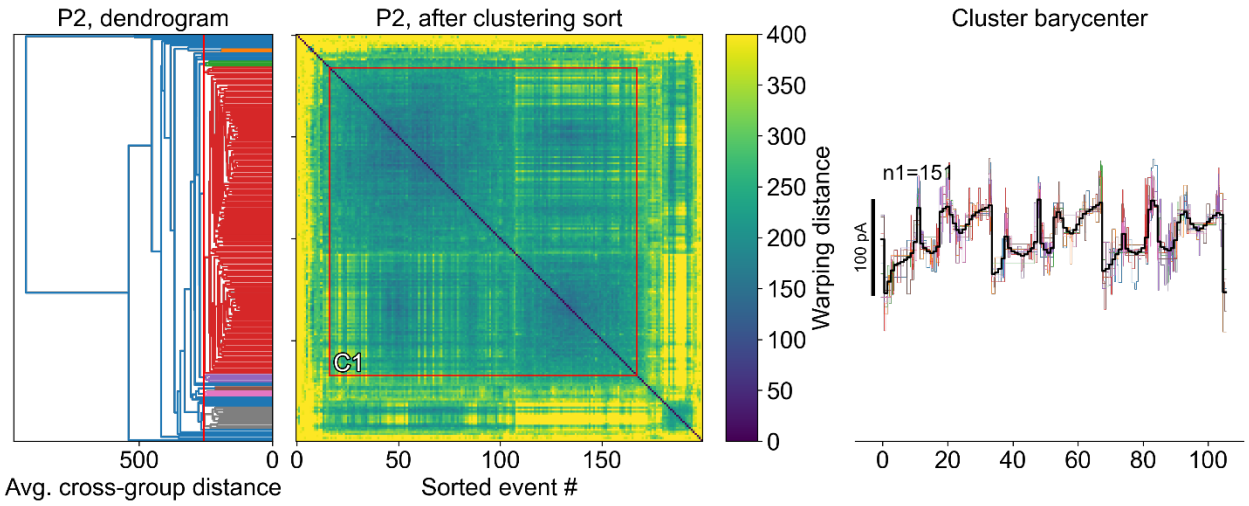

Figure S21. Clustering results on DTW Distance matrix of P2 Events and barycenters of clusters. Refer to Figure S19 for general description. Here, only one large cluster is formed under the same formation and filtration criteria. Based on the distance matrix, two clusters are observed here. For the sake of consistency, the same cut-point criterion based on 0.85th quantile of node distances was chosen, and therefore only one large cluster was formed.

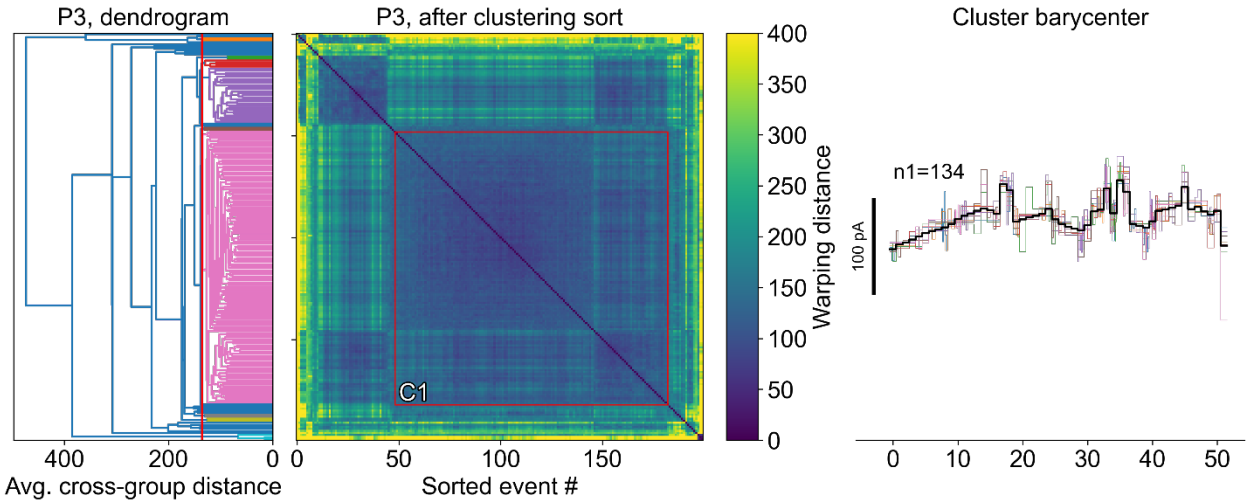

Figure S22. Clustering results on DTW Distance matrix of P3 Events and barycenters of clusters. Refer to Figure S19 for general description. Here, only one large cluster is formed under the same formation and filtration criteria. Based on the distance matrix, two or three clusters are observed here. For the sake of consistency, the same cut-point criterion based on 0.85th quantile of node distances was chosen, and therefore only one large cluster was formed.

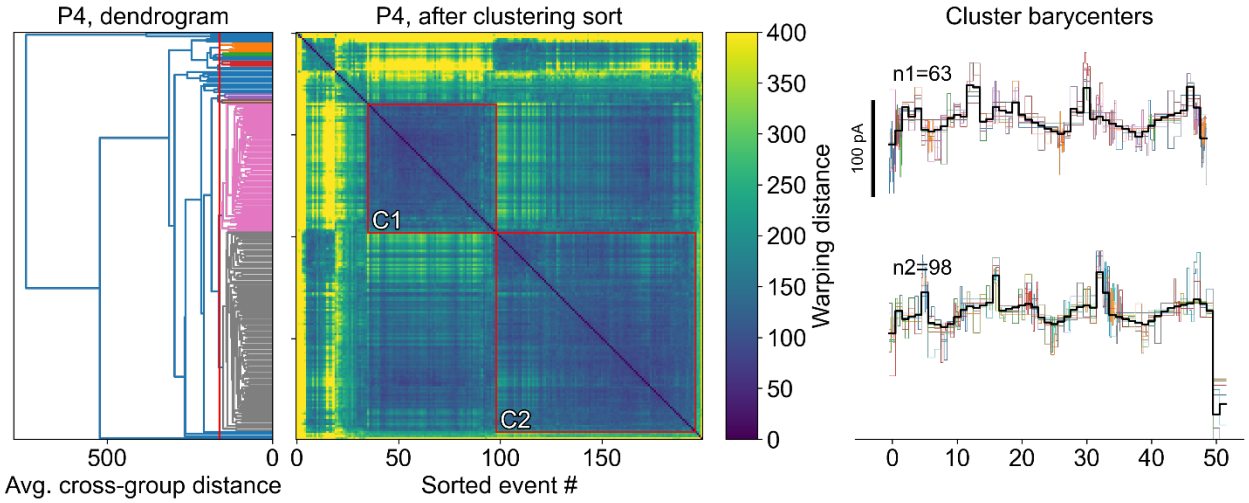

Figure S23. Clustering results on DTW Distance matrix of P4 Events and barycenters of clusters. Refer to Figure S19 for general description. Here, we see two large clusters, where similar to MBP clusters, the distinguishing feature is the presence or absence of the low-blockade level at the very end of the events.

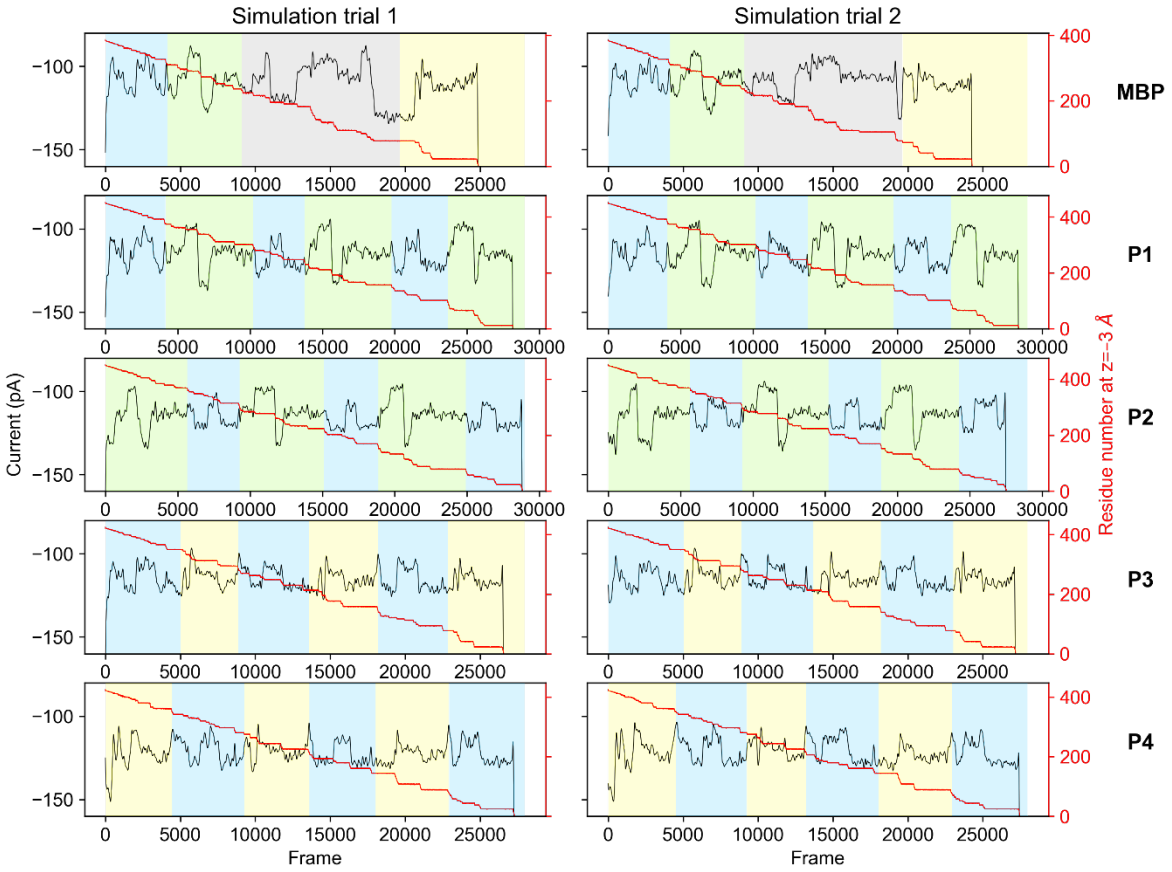

Figure S24. Two trials of multi-resolution simulation of full-length protein translocation and the resulting ionic current. Ionic current values, low-pass filtered with an 8th-order bidirectional Bessel filter with a cutoff-frequency of 50 frames, are shown in black. The translocation progression is displayed as residue number at z = −3Å (red line), and the corresponding sequence block is shown as colored rectangles in the background (refer to Figure 3a for color coding). The fuzzy transitions between the blocks are due to stalling and wobbling with an amplitude of roughly 1-9 aa residues.

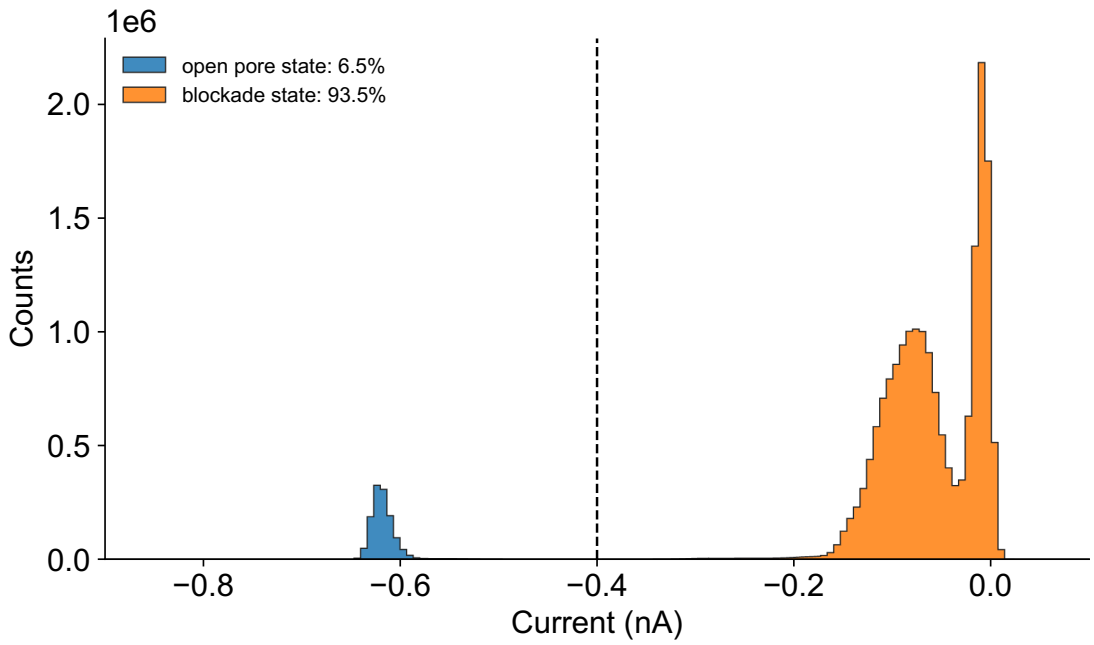

Figure S25. Total current distribution from high duty cycle measurements under saturated concentrations. Distribution of total samples from current trace of the 4-way PBI mixture experiment with a total protein concentration of ~120 nM (V = -300 mV). Histogram of the open (blue) and blocked (orange) states of CytK, with a dashed vertical line at -0.4 nA marking the threshold separating the two populations. The legend shows the relative occupancy (%) of each state, calculated from the total number of current samples.

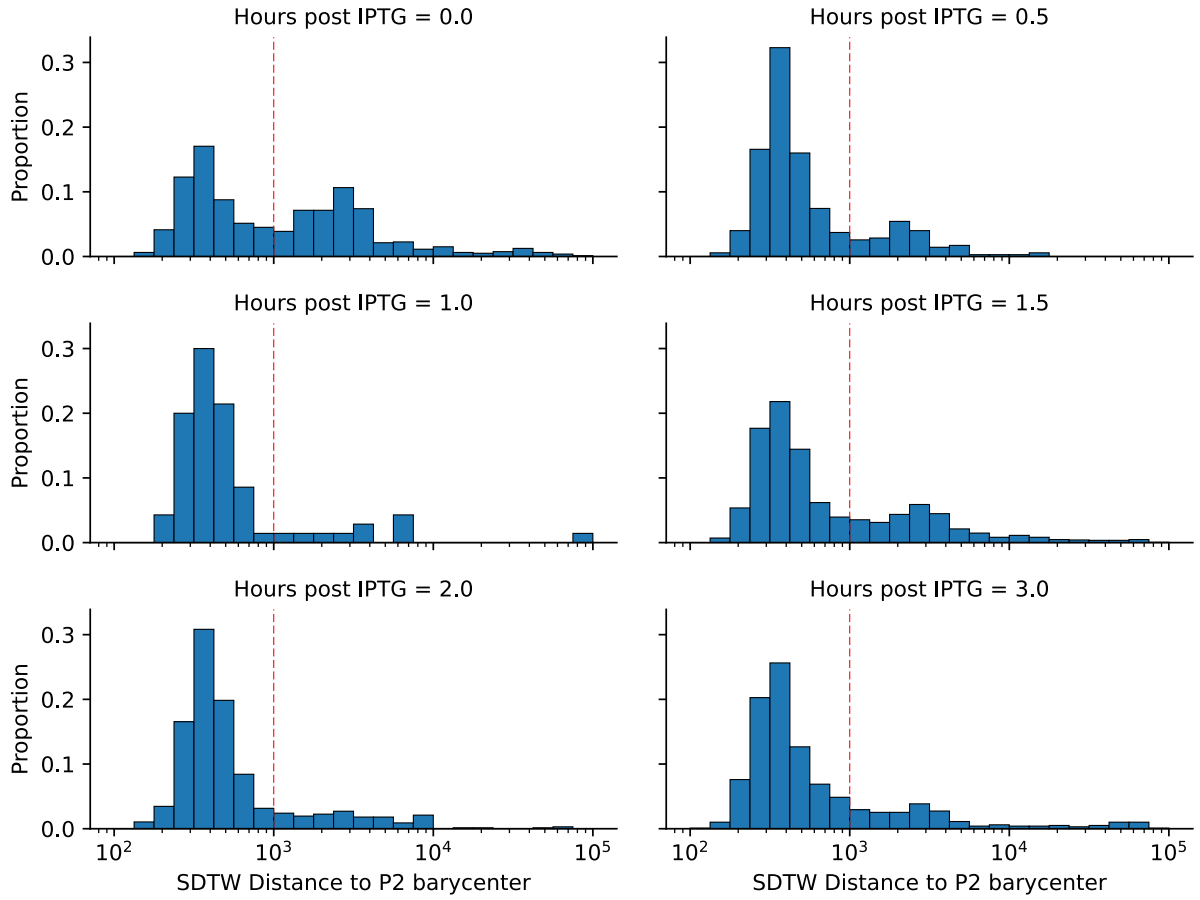

Figure S26. Soft-DTW score threshold used for discrimination of P2 translocations from background events in cell lysate. Histogram of Soft-DTW scores for all events after alignment to P2 barycenter signal reference at every induction time point. The red dashed vertical line in each plot denotes the P2 classification threshold, where events with a Soft-DTW alignment scores less than 1,000 were classified as P2. All experimental data were collected at -300 mV.

Sequences and plasmid designs for PBI analytes

To generate the PBI protein iterations (repeats of maltose binding protein, MBP, amino acids X-Y), plasmids encoding for PBIs were designed with codon-optimized DNA sequences that ensured repetitive protein segments had limited DNA sequence similarities while maintaining *Escherichia coli* codon frequency usage. Plasmids were ordered through Twist Bioscience. Prior to ordering plasmid designs, sequences were uploaded to Twist's online platform and designs flagged for any high repeat dense areas were further optimized using the Twist Codon Optimization tool.

Table 1: MBP and PBI analytes amino acid sequences.

Iteration	Amino acid sequence
MBP	MHHHHHHHHKIEEGKLVIWINGDKGYNGLAEVGKKFEKDTGIKVT VEHPDKLEEKFPQVAATGDGPDIIFWAHDRFGGYAQSGLLAEITP

6x His-tag (underlined) *segment 3 (yellow)* *segment U (gray)* *segment 2 (green)* *segment1 (blue)* *D10 tag (bold, red)*	DKAFQDKLYPFTWDAVRYNGKLIAYPIAVEALSLIYNKDLLPNPPK TWEEIPALDKELKAKGKSALMFNLQEPYFTWPLIAADGGYAFKYE NGKYDIKDVGVDNAGAKAGLTFLVDLIKNKHMNADTDYSIAEAAF NKGETAMTINGPWAWSNIDTSKVNYGVTVLPTFKGQPSKPFVGV LSAGINAASPNKELAKEFLENYLLTDEGLEAVNKDKPLGAVALKS YEEELAKDPRIAATMENAQKGEIMPNIPQMSAFWYAVRTAVINAA SGRQTVDEALKDAQTRITK**DDDDDDDDDD**
P1 *6x His-tag (underlined)* *segment 2 (green)* *segment1 (blue)* *D10 tag (bold, red)*	M<u>HHHHHHHHH</u>INGPWAWSNIDTSKVNYGVTVLPTFKGQPSKPFV GVLSAGINAASPNKELAKEFLENYLLTDEGLEAVNKDKPLGAVAL KSYEEELAKDPRIAATMENAQKGEIMPNIPQMSAFWYAVRTAVIN AASGRQTVDEALKDAQTRITKINGPWAWSNIDTSKVNYGVTVLPT FKGQPSKPFVGVLSAGINAASPNKELAKEFLENYLLTDEGLEAVN KDKPLGAVALKSYEEELAKDPRIAATMENAQKGEIMPNIPQMSAF WYAVRTAVINAASGRQTVDEALKDAQTRITKINGPWAWSNIDTSK VNYGVTVLPTFKGQPSKPFVGVLSAGINAASPNKELAKEFLENYL LTDEGLEAVNKDKPLGAVALKSYEEELAKDPRIAATMENAQKGEI MPNIPQMSAFWYAVRTAVINAASGRQTVDEALKDAQTRITK**DDD** **DDDDDDD**
P2 *6x His-tag (underlined)* *segment 1 (blue)* *segment 2 (green)* *D10 tag (bold, red)*	M<u>HHHHHHHHH</u>LKSYEEELAKDPRIAATMENAQKGEIMPNIPQMSA FWYAVRTAVINAASGRQTVDEALKDAQTRITKINGPWAWSNIDTS KVNYGVTVLPTFKGQPSKPFVGVLSAGINAASPNKELAKEFLENY LLTDEGLEAVNKDKPLGAVALKSYEEELAKDPRIAATMENAQKGE IMPNIPQMSAFWYAVRTAVINAASGRQTVDEALKDAQTRITKING PWAWSNIDTSKVNYGVTVLPTFKGQPSKPFVGVLSAGINAASPN KELAKEFLENYLLTDEGLEAVNKDKPLGAVALKSYEEELAKDPRIA ATMENAQKGEIMPNIPQMSAFWYAVRTAVINAASGRQTVDEALK DAQTRITKINGPWAWSNIDTSKVNYGVTVLPTFKGQPSKPFVGVL SAGINAASPNKELAKEFLENYLLTDEGLEAVNKDKPLGAVA**DDDD** **DDDDDD**
P3 *6x His-tag (underlined)* *segment 3 (yellow)* *segment 1 (blue)* *D10 tag (bold, red)*	M<u>HHHHHHHHH</u>KIEEGKLVIWINGDKGYNGLAEVGKKFEKDTGIKVT VEHPDKLEEKFPQVAATGDGPDIIFWAHDRFGGLKSYEEELAKD PRIAATMENAQKGEIMPNIPQMSAFWYAVRTAVINAASGRQTVD EALKDAQTRITKKIEEGKLVIWINGDKGYNGLAEVGKKFEKDTGIK VTVEHPDKLEEKFPQVAATGDGPDIIFWAHDRFGGLKSYEEELAK DPRIAATMENAQKGEIMPNIPQMSAFWYAVRTAVINAASGRQTV DEALKDAQTRITKKIEEGKLVIWINGDKGYNGLAEVGKKFEKDTGI KVTVEHPDKLEEKFPQVAATGDGPDIIFWAHDRFGGLKSYEEELA KDPRIAATMENAQKGEIMPNIPQMSAFWYAVRTAVINAASGRQT VDEALKDAQTRITK**DDDDDDDDDD**
P4 *6x His-tag (underlined)* *segment 1 (blue)* *segment 3 (yellow)* *D10 tag (bold, red)*	M<u>HHHHHHHHH</u>LKSYEEELAKDPRIAATMENAQKGEIMPNIPQMSA FWYAVRTAVINAASGRQTVDEALKDAQTRITKKIEEGKLVIWINGD KGYNGLAEVGKKFEKDTGIKVTVEHPDKLEEKFPQVAATGDGPDI IFWAHDRFGGLKSYEEELAKDPRIAATMENAQKGEIMPNIPQMSA FWYAVRTAVINAASGRQTVDEALKDAQTRITKKIEEGKLVIWINGD KGYNGLAEVGKKFEKDTGIKVTVEHPDKLEEKFPQVAATGDGPDI IFWAHDRFGGLKSYEEELAKDPRIAATMENAQKGEIMPNIPQMSA

	FWYAVRTAVINAASGRQTVDEALKDAQTRITKKIEEGKLVIWINGD KGYNGLAEVGKKFEKDTGIKVTVEHPDKLEEKFPQVAATGDGPDI IFWAHDRFGG**DDDDDDDDDD**

Table 2: MBP and PBI analytes DNA sequences.

Iteration	DNA sequence
MBP *6x His-tag (underlined)* *segment 3 (yellow)* *segment U (gray)* *segment 2 (green)* *segment1 (blue)*	ATGCATCACCATCATCATCACCATCACAAAATCGAAGAAGGTAAACT GGTAATCTGGATTAACGGCGATAAAGGCTATAACGGTCTCGCTGAA GTCGGTAAGAAATTCGAGAAAGATACCGGAATTAAAGTCACCGTTGA GCATCCGGATAAACTGGAAGAGAAATTCCCACAGGTTGCGGCAACT GGCGATGGCCCTGACATTATCTTCTGGGCACACGACCGCTTTGGTG GCTACGCTCAATCTGGCCTGTTGGCTGAAATCACCCCGGACAAAGC GTTCCAGGACAAGCTGTATCCGTTTACCTGGGATGCCGTACGTTAC AACGGCAAGCTGATTGCTTACCCGATCGCTGTTGAAGCGTTATCGC TGATTTATAACAAAGATCTGCTGCCGAACCCGCCAAAAACCTGGGAA GAGATCCCGGCGCTGGATAAAGAACTGAAAGCGAAAGGTAAGAGC GCGCTGATGTTCAACCTGCAAGAACCGTACTTCACCTGGCCGCTGA TTGCTGCTGACGGGGGTTATGCGTTCAAGTATGAAAACGGCAAGTA CGACATTAAAGACGTGGGCGTGGATAACGCTGGCGCGAAAGCGGG TCTGACCTTCCTGGTTGACCTGATTAAAAACAAACACATGAATGCAG ACACCGATTACTCCATCGCAGAAGCTGCCTTTAATAAAGGCGAAACA GCGATGACCATAAACGGTCCATGGGCATGGTCGAATATAGACACCT CTAAAGTGAATTACGGAGTAACCGTACTGCCCACGTTTAAAGGCCAA CCCTCAAAACCCTTTGTTGGGGTACTCTCAGCGGGAATTAACGCGG CCAGCCCGAATAAAGAACTCGCTAAGGAATTCCTTGAAAACTATCTC TTAACTGACGAAGGACTCGAAGCTGTTAACAAAGATAAACCTCTTGG GGCAGTTGCGCTTAAGTCTTATGAGGAAGAATTGGCAAAAGACCCC CGGATTGCGGCTACAATGGAAAATGCGCAGAAAGGGGAAATAATGC CGAATATACCGCAAATGTCAGCCTTTTGGTATGCCGTACGCACGGC GGTGATTAACGCAGCATCAGGACGCCAAACTGTCGATGAAGCTTTA AAAGATGCTCAAACAAGAATCACTAAA**GATGATGACGATGATGACG** **ACGATGATGAT**TAA
P1 *6x His-tag (underlined)* *segment 2 (green)* *segment 1 (blue)* *D10 tag (bold, red)*	ATGCATCACCATCATCATCACCATCACATAAATGGTCCCTGGGCCTG GAGCAATATAGATACTTCAAAGGTTAACTACGGAGTGACTGTTTTAC CAACATTTAAAGGACAGCCGTCTAAGCCCTTTGTGGGAGTTTTATCT GCTGGCATAAATGCAGCATCTCCAAATAAGGAATTGGCAAAGGAATT CTTGGAGAATTACTTGCTCACCGACGAGGGGTTGGAAGCAGTGAAC AAGGATAAGCCATTGGGAGCGGTCGCTCTTAAAAGTTATGAAGAGG AACTTGCAAAGGACCCGCGCATCGCAGCAACTATGGAGAATGCGCA AAAGGGCGAGATTATGCCAAATATTCCACAAATGAGCGCCTTTTGGT ACGCAGTTCGGACAGCAGTTATTAATGCGGCATCTGGCAGACAAAC CGTTGACGAGGCATTAAAGGATGCTCAAACCCGGATAACTAAAATCA ATGGACCGTGGGCCTGGTCTAACATAGATACCTCAAAAGTGAACTAT GGCGTAACCGTATTGCCGACCTTTAAAGGACAACCGTCAAAACCGT TTGTTGGCGTTTTAAGTGCAGGGATTAATGCAGCGTCTCCCAACAAA

	GAACTTGCCAAAGAATTTCTTGAAAACTACTTACTTACGGATGAGGG TTTAGAAGCAGTTAATAAAGATAAACCGCTTGGGGCGGTCGCGCTC AAAAGTTACGAAGAAGAGTTAGCTAAGGATCCCCGTATCGCGGCAA CCATGGAAAACGCACAAAAGGGAGAAATAATGCCGAACATACCCCA AATGAGTGCTTTCTGGTATGCAGTACGTACCGCGGTCATAAATGCC GCCTCAGGTCGTCAAACTGTGGATGAGGCACTTAAAGACGCTCAAA CCCGAATAACTAAAATAAACGGTCCATGGGCATGGTCGAATATAGAC ACCTCTAAAGTGAATTACGGAGTAACCGTACTGCCCACGTTTAAAGG CCAACCCTCAAAACCCTTTGTTGGGGTACTCTCAGCGGGAATTAAC GCGGCCAGCCCGAATAAAGAACTCGCTAAGGAATTCCTTGAAAACT ATCTCTTAACTGACGAAGGACTCGAAGCTGTTAACAAAGATAAACCT CTTGGGGCAGTTGCGCTTAAGTCTTATGAGGAAGAATTGGCAAAAG ACCCCCGGATTGCGGCTACAATGGAAAATGCGCAGAAAGGGGAAAT AATGCCGAATATACCGCAAATGTCAGCCTTTTGGTATGCCGTACGCA CGGCGGTGATTAACGCAGCATCAGGACGCCAAACTGTCGATGAAGC TTTAAAAGATGCTCAAACAAGAATCACTAAA**GATGATGACGATGATG** **ACGACGATGATGAT**TAA
P2 *6x His-tag (underlined) segment 1 (blue) segment 2 (green) D10 tag (bold, red)*	ATGCATCACCATCATCATCACCATCACCTGAAGTCTTACGAGGAAGA GTTGGCGAAAGATCCACGTATTGCCGCCACCATGGAAAACGCCCAG AAAGGTGAAATCATGCCGAACATCCCGCAGATGTCCGCTTTCTGGT ATGCCGTGCGTACTGCGGTGATCAACGCCGCCAGCGGTCGTCAGA CTGTCGATGAAGCCCTGAAAGACGCGCAGACTCGTATCACCAAGAT CAACGGCCCGTGGGCATGGTCCAACATCGACACCAGCAAAGTGAAT TATGGTGTAACGGTACTGCCGACCTTCAAGGGTCAACCATCCAAAC CGTTCGTTGGCGTGCTGAGCGCAGGTATTAACGCCGCCAGTCCGAA CAAAGAGCTGGCGAAAGAGTTCCTCGAAAACTATCTGCTGACTGAT GAAGGTCTGGAAGCGGTTAATAAAGACAAACCGCTGGGTGCCGTAG CGCTTAAATCTTACGAAGAAGAGCTTGCGAAGGATCCGCGTATCGC GGCCACTATGGAAAACGCCCAAAAGGGTGAAATAATGCCAAACATT CCTCAAATGTCGGCGTTTTGGTATGCAGTTCGTACAGCCGTCATAAA TGCGGCGAGCGGACGTCAAACTGTGGATGAGGCACTTAAAGACGC TCAAACCCGTATAACTAAAATAAATGGCCCCTGGGCGTGGTCTAACA TAGATACCTCAAAAGTAAACTATGGAGTTACAGTCTTACCTACATTTA AAGGGCAACCGAGCAAACCTTTTGTGGGAGTTCTGTCAGCCGGGAT TAATGCAGCGTCGCCAAACAAAGAATTAGCCAAAGAATTCTTGGAAA ACTACTTACTTACTGATGAGGGTTTAGAAGCCGTTAATAAAGATAAA CCCTTGGGTGCGGTAGCCTTGAAGTCCTATGAGGAAGAATTGGCGA AAGACCCACGCATAGCGGCGACTATGGAAAATGCTCAAAAGGGTGA AATTATGCCGAATATCCCGCAAATGTCAGCTTTCTGGTATGCGGTCC GGACAGCGGTAATTAACGCAGCCTCGGGGCGCCAAACTGTTGATGA AGCATTAAAAGATGCGCAAACTCGCATAACGAAAATCAACGGTCCAT GGGCTTGGAGTAATATAGACACAAGTAAAGTTAATTACGGAGTGACC GTTCTGCCCACCTTTAAAGGCCAACCCTCGAAACCGTTTGTTGGAGT TCTCAGCGCGGGAATAAACGCTGCCAGTCCCAATAAAGAACTGGCA AAGGAATTCCTTGAAAACTATCTCTTGACAGACGAAGGGCTCGAAG

	CGGTAAACAAAGATAAACCCCTGGGCGCTGTTGCA**GATGATGACGA** **TGATGACGACGATGATGAT**TAA
P3 *6x His-tag (underlined) segment 3 (yellow) segment 1 (blue) D10 tag (bold, red)*	ATGCATCACCATCATCATCACCATCACAAAATCGAAGAAGGTAAACT GGTAATCTGGATTAACGGCGATAAAGGCTATAACGGTCTCGCTGAA GTCGGTAAGAAATTCGAGAAAGATACCGGAATTAAAGTCACCGTTGA GCATCCGGATAAACTGGAAGAGAAATTCCCACAGGTTGCGGCAACT GGCGATGGCCCTGACATTATCTTCTGGGCACACGACCGCTTTGGTG GCCTGAAGTCTTACGAGGAAGAGTTGGCGAAAGATCCACGTATTGC CGCCACCATGGAAAACGCCCAGAAAGGTGAAATCATGCCGAACATC CCGCAGATGTCCGCTTTCTGGTATGCCGTGCGTACTGCGGTGATCA ACGCCGCCAGCGGTCGTCAGACTGTCGATGAAGCCCTGAAAGACG CGCAGACTCGTATCACCAAGAAGATTGAGGAAGGCAAGTTAGTTATT TGGATTAATGGTGATAAGGGCTACAATGGTCTGGCCGAGGTTGGCA AGAAATTTGAGAAGGACACTGGCATCAAAGTTACAGTCGAACACCC GGACAAATTGGAGGAGAAGTTCCCGCAAGTCGCAGCGACCGGTGA TGGTCCGGACATCATTTTTTGGGCTCATGACCGCTTCGGCGGCCTG AAGTCCTATGAGGAGGAACTGGCCAAAGACCCTCGCATTGCTGCTA CAATGGAGAATGCGCAGAAAGGCGAGATTATGCCTAATATCCCACA GATGTCTGCATTCTGGTACGCTGTCCGCACGGCTGTTATTAACGCA GCAAGTGGCCGCCAGACGGTTGACGAAGCTCTGAAGGATGCCCAG ACACGCATTACGAAGAAGATCGAGGAGGGTAAATTGGTCATTTGGA TCAACGGTGACAAGGGTTACAACGGCCTGGCAGAGGTAGGTAAGAA GTTTGAGAAAGACACAGGAATCAAGGTGACGGTAGAGCACCCAGAT AAGCTGGAGGAGAAATTTCCTCAAGTAGCTGCCACGGGCGACGGTC CTGATATAATCTTTTGGGCGCACGATCGCTTTGGCGGTCTGAAATCA TACGAAGAGGAGCTGGCTAAGGATCCTCGTATCGCAGCAACGATGG AGAACGCACAGAAGGGCGAGATCATGCCAAACATTCCTCAGATGAG CGCGTTCTGGTACGCAGTTCGTACCGCAGTCATCAATGCGGCGTCC GGCCGTCAGACCGTAGACGAGGCGCTGAAGGACGCACAGACCCGT ATTACAAAG**GATGATGACGATGATGACGACGATGATGAT**TAA
P4 *6x His-tag (underlined) segment 1 (blue) segment 3 (yellow) D10 tag (bold, red)*	ATGCATCACCATCATCATCACCATCACCTGAAGTCTTACGAGGAAGA GTTGGCGAAAGATCCACGTATTGCCGCCACCATGGAAAACGCCCAG AAAGGTGAAATCATGCCGAACATCCCGCAGATGTCCGCTTTCTGGT ATGCCGTGCGTACTGCGGTGATCAACGCCGCCAGCGGTCGTCAGA CTGTCGATGAAGCCCTGAAAGACGCGCAGACTCGTATCACCAAGAA AATCGAAGAAGGTAAACTGGTAATCTGGATTAACGGCGATAAAGGC TATAACGGTCTCGCTGAAGTCGGTAAGAAATTCGAGAAAGATACCG GAATTAAAGTCACCGTTGAGCATCCGGATAAACTGGAAGAGAAATTC CCACAGGTTGCGGCAACTGGCGATGGCCCTGACATTATCTTCTGGG CACACGACCGCTTTGGTGGCCTGAAGTCCTATGAGGAGGAACTGGC CAAAGACCCTCGCATTGCTGCTACAATGGAGAATGCGCAGAAAGGC GAGATTATGCCTAATATCCCACAGATGTCTGCATTCTGGTACGCTGT CCGCACGGCTGTTATTAACGCAGCAAGTGGCCGCCAGACGGTTGA CGAAGCTCTGAAGGATGCCCAGACACGCATTACGAAGAAGATTGAG GAAGGCAAGTTAGTTATTTGGATTAATGGTGATAAGGGCTACAATGG TCTGGCCGAGGTTGGCAAGAAATTTGAGAAGGACACTGGCATCAAA

	GTTACAGTCGAACACCCGGACAAATTGGAGGAGAAGTTCCCGCAAG TCGCAGCGACCGGTGATGGTCCGGACATCATTTTTTGGGCTCATGA CCGCTTCGGCGGCCTGAAATCATACGAAGAGGAGCTGGCTAAGGAT CCTCGTATCGCAGCAACGATGGAGAACGCACAGAAGGGCGAGATC ATGCCAAACATTCCTCAGATGAGCGCGTTCTGGTACGCAGTTCGTA CCGCAGTCATCAATGCGGCGTCCGGCCGTCAGACCGTAGACGAGG CGCTGAAGGACGCACAGACCCGTATTACAAAGAAGATCGAGGAGG GTAAATTGGTCATTTGGATCAACGGTGACAAGGGTTACAACGGCCT GGCAGAGGTAGGTAAGAAGTTTGAGAAAGACACAGGAATCAAGGTG ACGGTAGAGCACCCAGATAAGCTGGAGGAGAAATTTCCTCAAGTAG CTGCCACGGGCGACGGTCCTGATATAATCTTTTGGGCGCACGATCG CTTTGGCGGT**GATGATGACGATGATGACGACGATGATGAT**TAA

Table 3: MBP and PBI analytes normalized reverse capture rates ($nM^{-1}s^{-1}$) versus voltage.

Analyte	Cr at -150 mV	Cr at -200 mV	Cr at -250 mV	Cr at -300 mV
MBP	0.99±0.06	1.75±0.27	2.88±0.16	3.34±0.34
P1	0.41±0.03	2.47±1.05	3.17±0.6	3.72±1.61
P2	0.74±0.20	1.25±0.25	1.79±0.44	2.18±0.67
P3	1.36±0.06	1.87±0.35	2.77±0.62	3.36±0.43
P4	0.61±0.09	2.55±1.25	2.9±0.98	3.49±1.16

Table 4: Intact mass spectrometry results on PBIs.

Analyte	Expected Mass (kD)	Measured Mass (kD)
P1	49.6	49.6
P2	49.6	49.6
P3	47.6	47.6
P4	47.6	47.6

Table 5: Signal segment statistics for PBI analytes. Reported values are geometric means (μ_g) with their respective units and geometric standard deviations (σ_g) as unitless factors. To further clarify, μ_g is calculated as Exp(mean(ln(values))), and σ_g as Exp(S.D.(ln(values))).

Analyte	**MBP**	**P1**	**P2**	**P3**	**P4**
μ_g [Duration] (ms)	15.8	24.1	29.2	15.6	14.5
σ_g [Duration]	1.70	1.72	1.61	1.67	1.59
μ_g [Step Count]	60.7	95.3	115.3	58.6	55.5
σ_g [Step Count]	1.59	1.69	1.59	1.58	1.51
μ_g [Duration / Step Count] (μs/step)	260	253	254	267	262
σ_g [Duration / Step Count]	1.26	1.21	1.18	1.21	1.21
μ_g [Seq. Length / Step Count] (aa/step)	6.11	4.57	3.78	6.98	7.36
σ_g [Seq. Length / Step Count]	1.59	1.69	1.59	1.58	1.51